MODULAR NANOPARTICLES FOR SELECTIVE CELL TARGETING

A Thesis

Submitted to the Faculty

of

Purdue University

by

Kevin Peuler

In Partial Fulfillment of the

Requirements for the Degree

of

Master of Science in Biomedical Engineering

May 2019

Purdue University

Indianapolis, Indiana

THE PURDUE UNIVERSITY GRADUATE SCHOOL
STATEMENT OF THESIS APPROVAL

Dr. Chien-Chi Lin, Chair

Department of Biomedical Engineering

Dr. Mangilal Agarwal

Department of Mechanical and Energy Engineering

Dr. Michael C. Veronesi

Department of Radiology and Imaging Sciences

Approved by:

Dr. Julie Ji

Head of the Graduate Program

For my parents.

ACKNOWLEDGMENTS

I would like to thank my advisor, Dr. Chien-Chi Lin for his guidance and support throughout the course of my research and the thesis process. I truly appreciate the skills and knowledge I have gained in his laboratory.

I would like to thank my advisory committee members, Dr. Veronesi and Dr. Agarwal for their advice and time spent on of this thesis.

I would like to thank Integrated Nanosystems Development Institute (INDI) for use of their instrumentation.

I would also like to thank my colleagues: Mr. Hung-Yi (Gino) Liu, Mr. Matthew Arkenberge, Ms. Han Nguyen, Ms. Britney Hudson, Mr. Dustin Moore, Mr. Hunter Johnson, and Mr. Nathan Dimmitt for their support, friendship, and board game playing. A special thanks to Mrs. Sherry Clemens for her help with thesis formatting and assistance during my graduate studies.

I would like to thank my friends and family for their continued support throughout many aspects of my life. In particular, I would like to thank Jen Mackall for her support throughout my graduate studies.

TABLE OF CONTENTS

Page

Page

LIST OF TABLES

LIST OF FIGURES

Figure Page

LIST OF ABBREVIATIONS

5(6)-Fam	5(6)carboxyfluorescene
ANOVA	Analysis of Variance
Anti-2	Antibioticantimycotic
DAPI	4,6-diamidino-2-phenylindole
DCC	N,N-dicyclohexylcarbodiimide
DCM	Dichloromethane
DDH_2O	Double Distilled Water
DIC	Differential Interference Contrast
DLS	Dynamic Light Scattering
DMMB	Dimethylmethylene Blue
DS	Dextrin Sulfate
DTT	Dithiolthereitol
ECM	Extracellular Matrix
EDC	1-ethyl-3-(3-dimethylaminopropyl)carbodiimide
ELISA	Enzyme-Linked Immunosorbent Assay
FBS	Fetal Bovine Serum
$FDDH_2O$	Filtered Double Distilled Water
Hep	Heparin
IL	Interleukin
INFγ	Interferon Gamma
mTz	Methyltetrazine
LAP	Lithium Phenyl-2,4,6-trimethylbenzoylphosphinate
LPS	Lipopolysaccharide
NB	Norbornene

NHS	N-Hydroxysuccunimide
NP	Nanoparticle
PBS	Phosphate Buffer Solution
PEC	Polyelectrolyte Complex
PEG	Poly(ethylene glycol)
PEI	Polyethyleneimine
PLL	Poly-L-Lysine
RA	Rheumatoid Arthritis
RPM	Revolutions per Minute
SAM	Self-Assembled Monolayers
TAM	Tumor Associated Macrophage
TNF-α	Tumor Necrosis Factor Alpha
Tz	Tetrazine
UV	Ultraviolet

ABSTRACT

Peuler, Kevin M.S.B.M.E., Purdue University, May 2019. Modular Nanoparticles for Selective Cell Targeting. Major Professor: Chien-Chi Lin.

Nanoparticles (NPs) are an emerging technology in biomedical engineering with opportunities in diagnostics, imaging, and drug delivery. NPs can be prepared from a wide range of organic and/or inorganic materials. They can be fabricated to exhibit different characteristics for biomedical applications. The goal of this thesis was to develop NPs with tunable surface properties for selective cell targeting. Specifically, polyelectrolyte complexes composed of heparin (Hep, a growth factor binding glycosaminoglycan) and poly-L-lysine (PLL, a homopolymeric lysine) were prepared via a pulse sonication method. The Hep/PLL core NPs were further layered with additional Hep, tetrazine (Tz) modified Hep, or dextran sulfate (DS). The addition of Tz handle on Hep backbone permitted easy modification of NP surface with norbornene (NB) modified motifs/ligands, including inert poly(ethylene glycol) (PEG), cell adhesive peptides (e.g., RGD), and/or fluorescent marker. Both Hep and DS coated NPs could be readily internalized by J774A.1 monocytes/macrophages, whereas PEGylated NPs effectively reduced cellular uptake/recognition. The versatility of this NP system was further demonstrated by laying DS on the Hep/PLL NP surface. DS-coated NPs were recognized by J774A.1 cells more effectively. Furthermore, DS-layered NPs seemed to reduce IL-10 production on a per cell basis, suggesting that these NPs could be used to alter polarization of macrophages.

CHAPTER 1. INTRODUCTION

1.1 Biomedical Applications of Nanoparticles

Nanoparticle (NP) research is an accelerating field of study with promising work in diagnostics, imaging, and drug delivery. In diagnostics, NPs are used in microarray technology and acting as a biosensor for disease diagnosis. For example, You CC. et al. created a protein detection array based on gold nanoparticles that quench the fluorescence of the NP-bound probe (Figure 1.1A) [1]. The gold nanoparticle quenches fluorescent polymers that are bound to the nanoparticle via electrostatic interaction. Competitive binding by proteins release the fluorescent polymers. As a consequence, the fluorescent polymers are no longer quenched by the nanoparticle and can be quantitatively measured. An array composed of several nanoparticles with differing binding motifs is capable of detecting different proteins based on fluorescence signals.

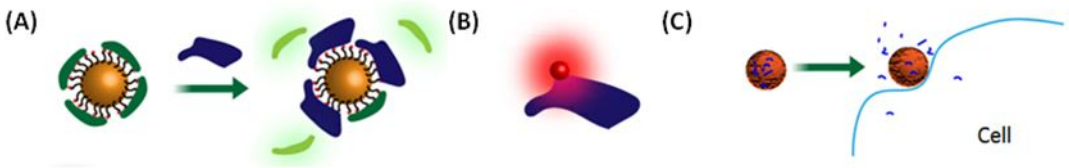

Fig. 1.1: A) Schematic representation of protein detection with gold nanoparticles. Gold nanoparticles quench green fluorescent strips, but upon binding with a protein (blue analyte) are released and capable of being measured. B) Schematic representation of a quantum dot tagged protein. C) Schematic representation of an NP delivering a drug to a cell.

For imaging, nano-scale quantum dots are used to label biological components, such as cells and proteins (Figure 1.1B). Quantum dots are photostable, hence allowing for real time monitoring of the movement of a biological component without concerns of photo bleaching. Additionally, NPs are being developed as contrasting agents for imaging applications, including nuclear magnetic resonance imaging (MRI), computed tomography (CT), positron emission tomography (PET), and ultrasound. The development of NPs for bio-imaging are with the intention to reduce the toxicity of current contrasting agents and increase the imaging time.

In drug delivery, NPs can serve as a drug carrier with tissue-targeting capability, which reduces off target adverse effects and the overall dosage of the drug delivered to the body. NPs also offer a method of cellular uptake of materials that otherwise would not be taken up, such as nucleic acids. Nucleic acids could be used for altering cellular activity, but a designed method for uptake is needed to bring these molecules into a cell, due to their very limited uptake by cells. For example, Lu et al. treated doxorubicin resistant breast cancer cells with a nanoparticle composed of anti-ABCB1 small interfering RNA complexed with poly(ethylene glycol) (PEG) modified and L-arginine oligo (alkylaminosiloxane) grafted PEI polyethyleneimine [2]. These NPs downregulated ABCB1 protein, enhancing doxorubicin uptake, which ultimately lead to increase cytotoxicity of the drug. Other biomedical applications of nanoparticles are shown in table 1.1.

Depending on the application and desired characteristics, NPs can be fabricated with organic materials (i.e. protein, polymer, lipids) or inorganic compounds (i.e. gold, silica, iron oxide). For drug delivery and cellular targeting, polymers are particularly advantageous due their biocompatability, ease of modification, and a wide range of natural and synthetic polymers are currently approved by the US Food and Drug Administration (FDA) for biomedical applications.

Table 1.1: Nanoparticle Materials and Fabrication Methods Employed for Biomedical Applications.

Materials	Fabrication Methods	Applications
Alloy (FePt, FeNi, FeCo, etc.)	Aerosol	Drug Delivery
Amphiphilic Molecules (Lipids)	Chemical	Bio-Imaging
Carbon Nanotubes	Emulsion	Bio-Sensing
Magnetic (Mn-Fe_2O_4, Fe_3O_4, γFe_2O_3, etc.)	Nucleation	Therapy (Gene, Cancer, Photothermal, etc.)
Metal Oxide (SiO_2, ZnO,TiO_2, etc.)	Laser Ablation	
Metallic (Au, Ag)	Self-Assemble (Electrostatic, micelle, lipid, etc.)	
Polymer (Natural, Synthetic)		
Silica (Mesopourous, Quantum dot)		

1.1.1 Fabrication of Nanoparticles

Various molecular interactions have been employed to fabricate nanoparticles. For example, amphiphilic molecules such as lipids are used to form liposomes and micelles. Amphiphilic molecules are composed of both hydrophobic and hydrophilic components. In solution, amphiphilic molecules can self-assemble into a monolayer or bilayer, forming micelles and liposomes respectively. In aqueous solution, amphiphilic molecules will minimize the interaction of the hydrophobic portion of the molecule with the polar solvent. As shown in Figure 1.2, amphiphilic molecules will align such that the hydrophilic portion of the molecules interacts with water while the hydrophobic portions are sequestered, thereby reducing its interactions with water. The hydrophobic portion can act as a cavity for carrying hydrophobic drugs, such as paclitaxel. For example, Nosrati et al. loaded hydrophobic artemisinin into a biodegradable micelle fabricated from a block copolymer composed of hydrophilic PEG and hydrophobic polycaprolactone (PCL) for treating breast cancer [3]. Biotin was conjugated to PEG and employed to target the over expressed biotin receptors on breast cancer cells. In a BALBc tumor model, the biotintilated, artemisinin loaded NPs were able to effectively target and significantly reduce tumor volume.

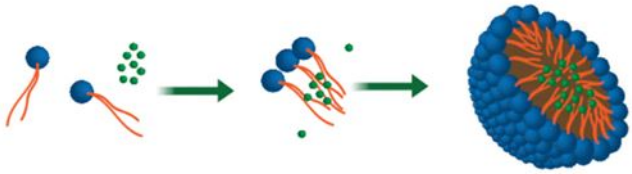

Fig. 1.2: Schematic representation of lipids forming a micelle with the blue polar head interfacing with polar solvent (i.e. water, acetonitrile, dimethyl sulfoxide) and the orange hydrophobic tail sequestered. The hydrophobic cavity made by the hydrophobic tails enable encapsulation of green hydrophobic drugs.

Hydrophobic interaction has also been employed for emulsion fabrication of nanoparticles. For example, a hydrophobic polymer can be dissolved in organic solvent (e.g., dichloromethane, DCM) and emulsified in aqueous solution. After collecting the NPs from the aqueous solution, DCM is allowed to evaporate and nano-scale polymer spheres are recovered.

Electrostatic interactions are employed for fabrication of polyelectrolyte complex (PEC) nanoparticles. The strong Coulombic force between negatively charged polyanions and positively charged polycations complex the polymers together, forming PEC NPs. Table 1.2 has some commonly used polymers for PEC NP fabrication. As shown in Figure 1.3, PECs can be generated by simple agitation, vortex, or sonication. NPs formed by electrostatic interactions are less prone to aggregation due to electrostatic repulsion from the surface charge. PEC NPs can complex with charged molecules, such as anionic nucleic acids for gene delivery applications. Utilization of charged polymers also permit facile modification/conjugation of nanoparticle surface with other functional moieties. Furthermore, formation of polyelectrolyte complex nanoparticles does not require additional crosslinking reagents. PEC NPs are also ideal for binding/complexing charged molecules, such as negatively charged nucleic acids [4, 5].

Table 1.2: Polymers commonly used for PEC nanoparticle synthesis.

Commonly Used Charged Polymers	
Polyanions	*Polycations*
Alginate	Chitosan
Carageenan	Poly-diallydimethylammonium
Cellulose Sulfate	Polyethylenimine
Dextrane Sulfate	Poly-L-lysine
Heparin	Protamine
Hyaluronic Acid	
Nucleic acid	
Polyacrylic acid	
Polystyrene sulfonic acid	

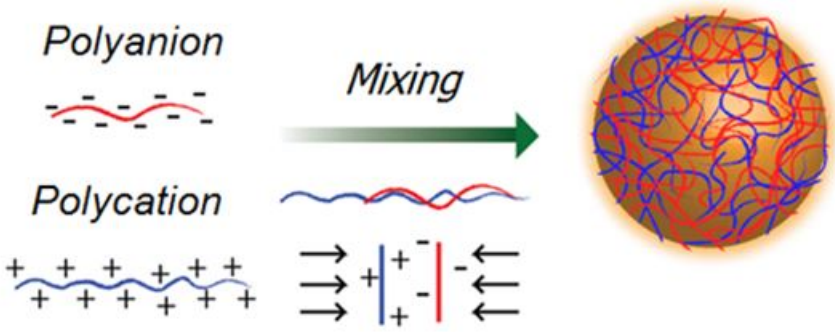

Fig. 1.3: Schematic representation of polyelectrolyte complex formation.

1.1.2 Heparin:Poly-L-Lysine Nanoparticles

Anionic heparin (Hep) and cationic poly-L-lysine (PLL) have been used to form self-assembled PEC nanoparticles. Anionic heparin (Hep) and cationic poly-L-lysine (PLL) have been used to form self-assembled PEC nanoparticles. Heparin (Figure 1.4A) is a naturally occurring glycosaminoglycan produced by mast cells. Heparin is widely used as an anticoagulant to treat thrombosis, heart attack, and pulmonary embolism. As a biomaterial, heparin is advantageous due to its affinity binding with

a wide range of growth factors [6]. In addition to growth factors, heparin also binds to extracellular matrix (ECM) proteins, plasma proteins, and enzymes [6].

PLL (Figure 1.4B) is a homopolymer polymerized by alpha amine of L-lysines. PLL has been used to coat contrasting agent nanoparticles to increase transfection efficiency for acoustical imaging and magnetic resonance imaging [7, 8]. PLL has also been employed to amplify signal for detecting amyloid , a potential biomarker for Alzheimer's Disease [9]. Additionally, PLL has been used to create variable viscoelastic nanotopographies, via laser interference lithography and layer-by-layer techniques to regulate stem cell behavior [10].

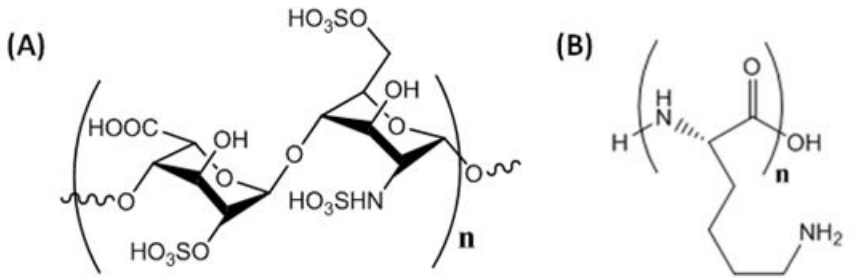

Fig. 1.4: A) Represented chemical structure of heparin. B) Chemical structure of poly-L-lysine.

Heparin/PLL nanoparticles have been used to improve biocompatibility of stents [11] and a cell delivery vehicle [12], as well as deliver laminin [13] and growth factors [14, 15]. Table 1.3 summarizes recent examples of heparin/PLL nanoparticles.

Table 1.3: Previously reported uses and preparation methods of hep/PLL nanoparticles [11–17].

Application	NP preparation method	Citation
Developed a cell delivery vehicle composed of PLGA microspheres coated with Hep/PLL nanoparticles.	Heparin was added to PLL in distilled water. Method of agitation was not provided.	[11]
Attached Hep/PLL NPs to dopamine coated surface to create a heparin gradient for studying the effect on platelet adhesion/activity and vascular cell growth.	Equal volumes of heparin and PLL solutions were added to the same container. 5min ultrasonic condition.	[12]
Hep/PLL NPs were attached to dopamine coated titanium for maintaining and regulating the intravascular biological response for stent implantation.	Equal volumes of heparin and PLL solutions were added to the same container. 5min ultrasonic condition.	[13]
Nerve growth factor and basic fibroblast growth factor loaded Hep/PLL NP used to improve treatment of peripheral nerve injury.	PLL solution was added dropwise to heparin solution while stirring, once complete it was stirred for 1hr at room temp.	[14]
VEGF loaded Hep/PLL NPs were immobilized on a dopamine coated titanium surface to inhibit platelet absorption and promoted epithelial cell proliferation	Equal volumes of VEGF and heparin were mixed and incubated for 1hr at 37°C. The mixture was added dropwise to PLL solution under ultrasonic condition.	[15]
Hep/PLL nanoparticles used for anti-thrombus activity. Red blood cells were used to transport the NPs, employing the attraction between the cell membrane charge and NP surface charge.	PLL and Heparin in solution were stirred for 24hrs.	[16]
Attached laminin loaded Hep/PLL NPs to dopamine coated titanium stent to block coagulation pathway and reduce thrombosis formation.	Laminin and heparin were mixed at equal volumes and incubated at 37C for 3hrs. Resulting solution was added dropwise to PLL under ultrasonic condition.	[17]

1.2 Surface Modification of Nanoparticles

Nanoparticle surface modification allows for compensation of shortcomings of the material used in fabrication, such as poor biocompatibility or propensity to aggregate. Surface modification also allows for the addition of functionality, such as covering the surface with PEG for cellular evasion. Gold NPs have been modified using self-assembled monolayers (SAMs) (Figure 1.5A). SAMs are formed by congregating organic molecules that have been absorbed onto the surface of a substrate. For example, the strong affinity between thiol and gold could be employed for the addition of thiol containing molecules onto a gold nanoparticle surface. NP surface can also be modified with an additional layer of polymers that have opposite charge to that of the underneath substrate (Figure 1.5B). This method is commonly employed for the addition of a more biocompatible material, such as heparin or hyualronic acid, which reduces cytotoxicity of cationic polymers.

In addition to physical adsorption, NP surface can be modified chemically with various methods, such as using carbodiimide coupling chemistry to conjugate carboxylic acid containing molecules onto a NP with surface primary amines. For example, Bramberger et al. reduced spleen cell binding of particles by modifying nanoparticles' surface with PEG via reacting N-Hydroxysuccunimide (NHS) modified PEG to NP surface amines [18]. The binding between biological components, such as biotin and avidin can also be employed for NP surface modification. For example, Matsumura et al. conjugated monoclonal antibodies, via biotin-avidin binding onto the surface of a metal-latex nanocomposites. Consequently, the nanocomposite acted as a detection probe for influenza virus [19].

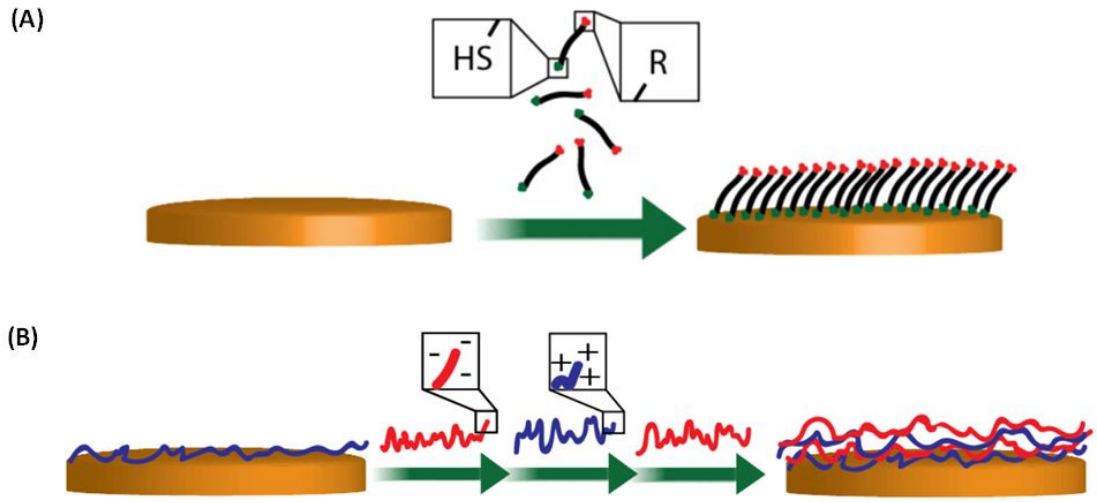

Fig. 1.5: A) Schematic representation of self assembled monolayer addition onto a gold substrate. The green thiol affixes to the gold surface and the red functional group is separated by an alkyl chain. B) Schematic representation of layering-by-layer addition of oppositely charged polymers on a surface.

Adding functionality is of great importance for targeting, tracking, and cellular evasion or uptake. Conjugating a handle on NP surface permits further attachment of modified peptides, fluorescent tag, antibody, and polymers (e.g., PEG), as shown in Figure 1.6. Attaching an antibody to the NP surface could improve binding of NPs to specific receptors on cell surface. On the other hand, modifying a NP surface with PEG, a technique termed PEGylation, effectively reduces non-specific cellular uptake and increases plasma circulation time [18, 20–22]. For example, Viard, M., et al. modified phospholipid based nanostructure with PEG to improve circulation time and efficacy of cancer treatment [23]. Another approach to prevent non-specific clearance is through addition of CD-47 protein onto the NP surface [24]. CD-47 protein can provide cellular evasion by signaling to the cell that the NP is not a foreign entity [24].

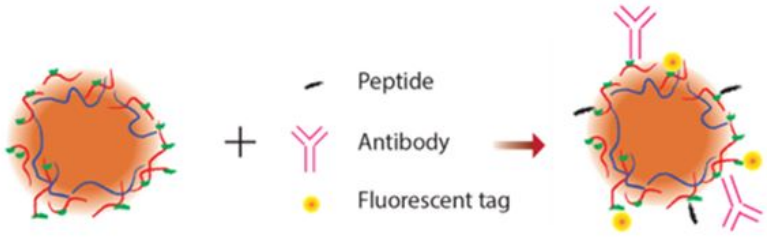

Fig. 1.6: Schematic representation of nanoparticle surface modification.

1.2.1 Tetrazine-Norbornene Click Chemistry

Click reactions offer powerful options for functionalization of polymers and nanoparticles. Proceeding without addition of catalysts or altering pH, click reactions can functionalize materials without worrying about side reactions and altering the electrostatic interaction in the nanoparticle. Tetrazine(Tz):norbornene(NB) reaction, shown in Figure 1.7 is a bioorthogonal click reaction capable of spontaneous reaction with each other without reacting with other molecules in the body. Jivan et al. employed Tz:NB click reaction to tethered glucose oxidase onto a microparticle without losing enzyme bioactivity [25]. Han et al. used Tz:NB click chemistry to labeled epidermal growth factors with quantum dots in order to label human skin cancer cell, which over expresses epidermal growth factor receptors [26]. Han et al. utilized Tz:NB click reaction to label quantum dots with antibodies for in vivo single cell labeling [27].

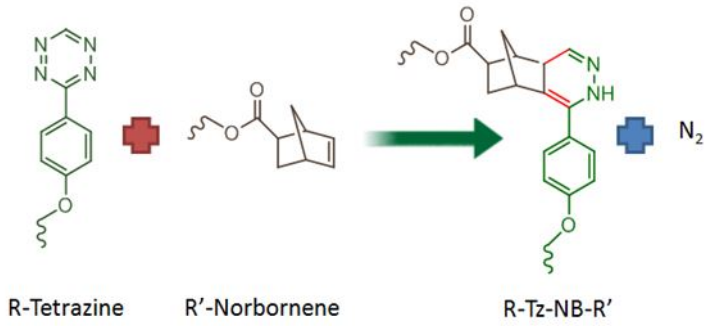

Fig. 1.7: Schematic representation of tetrazine-norbornene reaction.

1.3 Nanoparticle-Induced Macrophage Polarization

As part of the immune system, macrophages play an important role in eliminating foreign materials, cellular debris, bacteria, pathogens, and cancer cells through phagocytosis. Macrophages also elicit inflammatory response through secretion of cytokines. Macrophages are generally categorized into M1 and M2 phenotypes. M1 macrophage are activated to defend against viral and bacterial infections. M1 macrophages perform phagocytosis of foreign entities and are responsible for releasing proteases and pro-inflammatory cytokines, including interleukin 1 (IL-1), IL-6, and tumor necrosis factor alpha (TNF-α). M1 macrophages can be activated through the administration of lipopolysaccharide (LPS) or interferon gamma (INF-γ). M2 macrophages are anti-inflammatory. They are responsible for removing cellular debris while eliciting an anti-inflammatory environment with the production of cytokines, such as IL-10, and TNF-β. M2 macrophages can be activated through the administration of IL-4 and IL-13.

Due to the macrophages ability to influence the local environment, influencing macrophage activation state could offer a control of the inflammation of the local environment. This potential influence over inflammation could prove beneficial for treatment of diseases affecting inflammation, such as arthritis. Influencing macrophage cytokine production could also influence response from other immune cells which could be beneficial for treating cancer. In general, modulation of macrophage phenotype could prove beneficial for disease treatment. For example, Huang et al. demonstrated ethylenediamine conjugated dextran and polyethylenimine (PEI) repolarized tumor-associated macrophages (TAMs) from M2 to M1 phenotypes for cancer immunotherapy [28]. TAMs are immune cells that have been influenced by the tumor environment to exhibit M2 like tendencies and have been shown to increase metastasis, proliferation, and angiogenesis of various tumors. The repolarized macrophages from the PEI or ethylenediamine conjugated dextran treatment secreted more IL-12, which stimulates natural killer cells and natural killer T cell. Furthermore, PEI and

ethylenediamine modified dextran elicited an immune response through the TAMs and successfully reduced tumor size. In another example, Kim et al. treated rheumatoid arthritis (RA) by modulating M1/M2 population with nanoparticles decorated with manganese ferrite and ceria [29]. RA is an autoimmune disease with increased inflammation of the synovial fluid, eventually leading to a breakdown of cartilage and bone. It was found that hypoxia and reactive oxygen species (ROS) play a large role in shifting macrophage polarization from M2 to M1 phenotype, leading to a pro-inflammatory environment in RA. Furthermore, manganese ferrite and ceria nanoparticles scavenge ROS and produce oxygen, leading to repolarization of M1 to M2 macrophage and this repolarization reduced inflammation and promoted recovery of the arthritic site.

To influence macrophage phenotypes, NPs can be employed to increase uptake of a material (drug, nucleic acid, polymer, etc.) while providing targeting capabilities, thereby improving treatment efficacy while reducing off target adverse effects.

CHAPTER 2. OBJECTIVES

2.1 Overview

The overall goal of this thesis was to develop a nanoparticle system whose surface properties can be modularly controlled. Ideally, these modular NPs can be modified to exhibit a wide range of surface properties for targeting specific areas of the body and to elicit a change in cellular behaviors. Here, a modular NP scaffold was fabricated to afford facile tagging of biomacromolecules (e.g., glycosaminoglycans or GAGs, peptides, antibodies, fluorophores, etc.) for selective cell targeting. In particular, ultrasonication was employed for fabricating both the core NP scaffold and the surface coating. Compared with vortexing or mechanical agitation, ultrasonication provides stringent controls in synthesis conditions, which should produce NPs with more reproducible sizes or narrower size distribution. In addition to layering NPs with different GAGs, this thesis work also explored bioorthogonal click chemistry to modify NP surface. Specifically, modular reactivity of tetrazine-modified NP surface with norbornene-conjugated molecules was beneficial for altering cell targeting capability. Finally, the utilities of the fabricated modular NPs were demonstrated using selective targeting of macrophages in vitro.

2.2 Objective 1: Development of Modular Nanoparticle System

The first objective of this thesis was to develop heparin/PLL NPs with modular compositions and surface functionality. Specific tasks to accomplish this goal were:

- To establish a two-step ultrasonication protocol for forming core-shell heparin/PLL nanoparticles.
- To construct NPs with various surface coating of GAGs (e.g., heparin, dextran sulfate).
- To demonstrate biorthogonal NP surface modification via norbornene-tetrazine click chemistry.

2.3 Objective 2: Investigation of the Effect of Nanoparticles on Cellular Uptake and the Polarization of Monocyte

The second objective of this thesis was to demonstrate the modular NPs can be used to control cellular uptake and inflammatory cytokine production. Specific tasks to accomplish this goal were:

- To test cytocompatibliity of the modular NPs.
- To examine the effect of NP modification on cellular uptake/recognition.
- To determine the effect of dextran sulfate coated NPs on IL-10 production from J774A.1 cells.

CHAPTER 3. MATERIALS AND METHODS

3.1 Materials

Poly-L-lysine hydrobromide (PLL, 120 kDa) was purchased from Polysciences Inc. Heparin sodium (Hep, 16.3 kDa) was purchased from Celsus Laboratories. Eight-arm PEG-OH (20 kDa) was purchased from JenKem Technology, USA. tetrazine-PEG5-NHS ester, dithiolthereitol (DTT), deuterium oxide, sodium chloride, 1,9-dimethylmethylene blue zinc chloride double salt, N,N-dicyclohexylcarbodiimide (DCC), 4-(dimethylamino)pyridine (DMAP), Norbornene-2-carboxylic acid, and diethyl ether were purchased from Sigma-Aldrich. Acetic Acid was purchased from VWR Chemicals. Tetrazine amine, methyltetrazine amine, methyltetrazine-PEG4-amine were purchased from Click Chemistry Tools. Dextran sulfate sodium salt (DS, 40 kDa) was purchased from Alfa Aesar. 1-ethyl-3-(3-dimethylaminopropyl)carbodiimide (EDC) and N, N-Diisopropylethylamine were purchased from TCI. N-Hydroxysuccunimide (NHS), phenol, and N,N,Dimethylformamide (DMF) were purchased from Acros Organics. Lipopolysaccharide (LPS) was purchased from Cell Signaling Technology. Paraformaldehyde was purchased from Macron Chemical. Dulbeccos modified eagle medium (DMEM), fetal bovine serum (FBS), Dulbeccos Phosphate Buffered Saline (DPBS), and 100X antibioticantimycotic (anti-2) were purchased from Hyclone. Saponin was purchased from Chem-impex International Inc. 4",6-Diamidino-2-phenylindole, dihydrochloride (DAPI) was purchased from Anaspec Inc. Fmoc-protected amino acids, 1-[Bis(dimethylamino)methylene]-1H-1,2,3-triazolo[4,5-b] pyridinium 3-oxid hexafluorophosphate, hexafluorophosphate azabenzotriazole tetramethyl uronium (HATU), N,N,N,N -tetramethyl-O-(1H -benzotriazol-1-yl)uronium hex-

afluorphosphate (HBTU),and hydroxybenzotriazole (HOBt) were purchased from either Anaspec or ChemPep. Frifluoroacetic acid was attained from EMD. Sulfo-Cy5-tetrazine was purchased from Santa Cruz Biotechnology.

3.2 Material Synthesis

3.2.1 Methyltetrazine or Tetrazine Modified Heparin

Heparin modifications employed standard carbodiimide crosslinker chemistry. Heparin sodium salt was dissolved at room temperature in ddH_2O with stirring. 5-fold excess of EDC and NHS were then added to heparin solution and stirred at room temperature for 30 minutes. In a separate container, 5 fold excess of methyltetrazine-amine, tetrazine-amine, or methyltetrazine-PEG4-amine was dissolved in ddH_2O and kept from light. Once the 30minutes were complete, the solutions were combined and stirred in the dark, over night. To purify the modified heparin, dialysis was performed on the resulting solution (3500 MWCO) at room temperature for two days in ddH_2O and then lyophilized. Substitution was determined against a standard curve of mTz-amine, Tz-amine, or mTz-PEG4-amine via Synergy HT microplate reader at absorbance 523nm.

3.2.2 5(6) Carboxyfluorescene Modified Poly-L-Lysine

Modification of poly-L-lysine utilized carbodiimide crosslinker chemistry. 2 Fold excess (compared to PLL) of 5(6) Caboxyfluorescene was dissolved at room temperature in ddH_2O with stirring and kept from light. 5-fold excess (compared to PLL) of EDC and NHS was then added to 5(6)caboxyfluorescene solution and stirred at room temperature for 30 minutes, while kept from light. In a separate container, poly-L-lysine hydrobromide was dissolved in ddH_2O and kept from light. Once the 30 minutes were complete, the solutions were combined, pH was adjusted to 6.8, and stirred in the dark for 5 hours. To purify the modified PLL, dialysis was performed

on the resulting solution (6-8kDa MWCO) at room temperature for two days ddH_2O and then lyophilized.

3.2.3 Photoinitiator LAP

Photoinitiator Lithium Phenyl-2,4,6-trimethylbenzoylphosphinate (LAP) was synthesized according to previously reported method [30].

3.2.4 Norbornene Modified GGGRGDS Peptide

GGGRGDS synthesis was performed via standard Fmoc coupling chemistry in an automated, microwave-assisted peptide synthesizer (Liberty 1, CEM). The crude products were cleaved from resin in a solution consisting of 2.5% ddH_2O, 2.5% Tri-sisopropylsilane, 95% trifluoroacetic acid, and 5% (w/v) phenol for 3 hours at room temperature. The crude peptides were precipitated in cold ethyl ether and dried in a desiccator. The dried peptides were purified using HPLC (Flexar system, Perkin Elmer) and confirmed by mass spectrometry (QTOF, Agilent Technologies).

NB-GGGRGDS was synthesized via 1-[Bis(dimethylamino)methylene]-1H-1,2,3-triazolo[4,5-b]pyridinium 3-oxid hexafluorophosphate, Hexafluorophosphate Azabenzotriazole Tetramethyl Uronium (HATU) coupling reaction. 5-norbornene-2-carboxylic acid (5 fold molar excess to peptide, 5X), HATU (5X), and 3 mL DMF were added to a flask and stirred, via magnetic stir bar. N, N-Diisopropylethylamine (DIEA, 5.1X) was added to the solution and stirred for 3 minutes. The resulting activated norbornene acid was added to a flask containing purified GGGRGDS in DMF and allowed to react for 3 hours at room temperature, under stirring. The NB-GGGRGDS product was precipitated in cold diethyl ether and dried in a desiccator.

3.2.5 PEG Macromer

Methyl-PEG-NB, two arm PEG-diNB, and eight arm PEG-norbornene were synthesized according to a previously reported method with minor modifications [31]. For example, eight-arm PEG-norbornene (PEG8NB, 20 kDa) was synthesized as follows. 5-norbornene-2- carboxylic acid (5-fold molar excess to eight arm PEG-OH(PEG8OH) hydroxyl groups(5X)) was reacted with DCC (2.5X) for 1 hour in anhydrous DCM, resulting in norbornene anhydride. In a separate two-necked round bottom flask PEG8OH, DMAP (0.5X), and pyradine (0.5X) were mixed with DCM under nitrogen. Upon completion of the hour, the norbornene anhydride was filtered to remove by-products and added dropwise via addition funnel to the separate two-necked round bottom flask containing PEG8OH while under nitrogen. The flask was removed from light and the reaction was allowed to proceed overnight. The process was repeated to improve norbornene functionalization of the PEG. The PEG8NB product was precipitated in cold diethyl ether and dried in a desiccator. The dried product was dissolved in ddH_2O and dialyzed for 3 days at room temperature (6-8 kDa MWCO), followed by lyophilization. ^{1}H NMR (Bruker Advance 500) was used to determine the degree of PEG functionalization.

3.2.6 Linear Cy5-PEG-NB

Linear Cy5-PEG-NB was synthesized by mixing PEG-diNB (6kDa) with Cy5-Tz for 1 hour. A NB/Tz ratio of 20 was used to ensure conjugation of Cy5-Tz to PEG-diNB.

3.3 One-Step Nanoparticle Preparation

Specific volume of PLL dissolved in filtered (0.22mum PVDF) double distilled water (fddH_2O) was added to a test tube, followed by the addition of fddH_2O, and an aliquot of heparin dissolved in fddH_2O. Total volume of 2mL was used for initial

testing. The solution was sonicated using a Bronson Digital Sonifier at 19.9500.100 kHz, with 10% amplitude, for an initial duration of 5 minutes with the test tube in ice water. For pulse sonication one step preparation, after the initial 5 minutes, a 10 min cool down period, followed by 2.5 min sonication, followed by 2 min cool down, and 2.5min sonication.

The resulting solution was analyzed by dynamic light scanning via Malvern Zetasizer Nano ZS90. The zeta potential was measured using Zetasizer Nano Series disposable folded capillary cells. Nanoparticle size was measured utilizing UV-disposable cuvettes.

3.4 Two-Step Nanoparticle Preparation

Separately, PLL, dextran sulfate, and heparin were dissolved in filtered (0.22mum PVDF) double distilled water (fddH_2O). Specific volume of PLL solution was added to a test tube, followed by the addition of fddH_2O, and an aliquot of heparin solution. The ratio of Hep/PLL was 0.7 and the total volume of 2mL was used. 0.25mg/mL PLL and 0.175mg/mL heparin were used for Hep/PLL ratio of 0.7. The solution was sonicated using a Bronson Digital Sonifier at 19.9500.100 kHz, with 10% amplitude, for an initial duration of 5 minutes. After around 8min of cooling down the solution, additional material (Heparin, Heparin-Tz, heparin-mTz, Dextrin Sulfate) was added to bring the ratio of Hep+additional material/PLL to 1.3. After the 10min cool down, the solution was sonicated for 2.5min, followed by 2min cool down, and 2.5min sonication.

The resulting solution was analyzed by dynamic light scanning via Zetasizer Nano. The zeta potential was measured using Zetasizer Nano Series disposable folded capillary cells. The size was measured utilizing UV-disposable cuvettes.

3.5 Nanoparticle Stability

Nanoparticles were measured via Zetasizer Nano with UV-disposable cuvettes over the course of a month.

Dimethyl methylene blue assay was performed as follows. DMMB solution was prepped by first adding 16mg 1,9-deimethyl-methylene blue zinc chloride into 1L of double distilled water containing 3.04g glycine, 1.6g sodium chloride, and 95mL of 0.1M acetic acid. The solution was then stirred and kept from light. A heparin standard curve was prepared with concentrations from 40mug/mL to 5ug/mL with a blank. 20muL of standards and samples were added to a 96 well plate. 180muL DMMB solution was added to each well and the plate was measured by a Synergy HT microplate reader via absorbance at 530nm.

3.6 Monitoring Heparin-mTz:Methyl-PEG-NB Reaction by ^{1}H NMR

Methyl-PEG-NB and mTz-heparin were dissolved separately in deuterium oxide. The solutions were mixed together, added to an NMR tube, and measured via ^{1}H NMR (Bruker Advance 500). A 3:2 ratio of mTz:NB was used.

3.7 Cy5 NPs and NP Hydrogel Hybrid

Tz-heparin coated nanoparticles and linear Cy5-PEG-NB at a Tz:NB ratio of 1:1 were mixed for 24hours. Once mixing was complete, the solution was centrifuged for 25 minutes at 14,000 RPM. The supernatant was removed and the pellet was resuspended in ddH_2O. This step was repeated two more time to remove excess Cy5-PEG-NB. Solution was placed in bath sonicator for 5min.

PEG8NB (3wt%), Cy5-PEG-NPs (7.3wt%), and PBS were kept from light and mixed for 24hrs. Desired amounts of DTT, with a thiol/ene ratio of 0.9 and LAP (1mM) photoinitiator were mixed in and the resulting solution was injected between two slides, separated with 1mm Teflon spacers. The solutions were then subjected

to 365nm light (5 mW/cm2) for 2 minutes. Resulting gels were transferred to PBS, kept from light, and allowed to swell prior to confocal imaging.

3.8 Cell Viability

J774A.1 cells were seeded (5,000 cells per well) into a 96 well plate. Cells were treated with varying concentrations of PLL, Hep, DS, and 1.3 Hep/PLL NPs. Cells were confluent at the time of measurement. For the NP study, equal concentration of PLL was in solution as within the NP. Cells were incubated for 3 hrs followed by administration of sterile 0.4mg/mL thiazolyl blue tetrazolium bromide solution in serum free DMEM high glucose media and removed from light. Solution was incubated at 37^oC for 2 hours. Upon completion of incubation, $120mu$L of DMSO was added. The solution was mixed and $100mu$L was transferred to a 96 well plate for reading on microplate reader with a 570nm wavelength.

3.9 Nanoparticle Uptake by 3T3 and J774A.1 Cells

First, 75,000 J774A.1 cells were seeded on 35mm tissue culture plates. Non-activated cells are allowed to culture in DMEM high glucose culture media with 10% fetal bovine serum and 1% antibioticantimycotic (anti-2) for 3 days before nanoparticle administration. Activated cells were allowed to culture for 2 days followed by administration of $1mu$g/mL lipopolysaccharide (LPS) and allowed to culture for 1 day before nanoparticle administration. Two step nanoparticles were prepared with dextran sulfate, heparin, or Tz-heparin coating. NPs were prepared with 0.25mg/mL PLL-5,6-carboxyfluorescene. Tz-Heparin coated nanoparticles were mixed with one arm linear PEGNB (5.5 NB:Tz) for 24 hours. Heparin and dextran sulfate coated NPs were mixed with an equal volume of fddH_2O for 24 hours. A mixture of 10% sterile NP solution and 90% media was administered to the cells for 4 hours. Upon completion of the 4 hours, media was removed and cells were fixed with 4% paraformaldehyde, treated with saponin, and stained with DAPI. Images were taken with a confocal mi-

croscope (Olympus Fluoview FV100 laser scanning microscope), with DAPI used to focus the image. Images were quantified by ImageJ by measuring the mean intensity of the FITC image and counting cells of the DAPI image.

100,000 3T3 cells were seeded on 35mm tissue culture plates. Cells were cultured for 3 days in DMEM high glucose culture media with 10% fetal bovine serum (FBS) and 1% anti-2 for 3 days before nanoparticle administration. Two step nanoparticles were prepared with dextran sulfate, heparin, or Tz-heparin coating. NPs were prepared with 0.25mg/mL PLL-5,6-carboxyfluorescene. Tz-heparin coated nanoparticles were mixed with one arm linear PEGNB (5.5 NB:Tz) for 24 hours. Heparin and dextran sulfate coated NPs were mixed with an equal volume of fddH_2O for 24 hours. A mixture of 10% sterile NP solution and 90% media was administered to the cells for 4 hours. Upon completion of the 4 hours, media was removed and cells were fixed with 4% paraformaldehyde, treated with saponin, and stained with DAPI. Images were taken with a confocal microscope, with DAPI used to focus the image. Images were quantified by ImageJ by measuring the mean intensity of the FITC image and counting cells of the DAPI image.

3.10 RGD-Bound Nanoparticle Recognition by 3T3 Fibroblast Cells

100,000 3T3 cells were seeded on 35mm tissue culture plates. Cells were cultured for 3 days in DMEM high glucose culture media with 10% fetal bovine serum (FBS) and 1% anti-2 for 3 days before nanoparticle administration. Two step nanoparticles were prepared with dextran sulfate, heparin, or Tz-heparin coating. NPs were prepared with 0.25mg/mL PLL-5,6-carboxyfluorescene. Tz-heparin coated nanoparticles were mixed with NB-GGGRGDS peptide (10:1 peptide:Tz) for 24 hours. Heparin coated NPs were mixed with an equal volume of fddH_2O for 24 hours. A mixture of 10% sterile NP solution and 90% media was administered to the cells for 4r hours. Upon completion of the 4 hours, media was removed and cells were fixed with 4%

paraformaldehyde, treated with saponin, and stained with DAPI. Images were taken with a confocal microscope, with DAPI used to focus the image.

3.11 Effect of NPs on LPS Treated Cells

100,000 J774A.1 cells were seeded on 35mm tissue culture plates. Cells were cultured with DMEM high glucose media (10% FBS, 1% anti-2). After 24 hours, LPS ($1mu$g/mL) in media (1.2mL) was administered to the plate. After an additional 24 hours, a 1.2mL solution of 10% NP/Soluble DS/fddH_2O in media was administered. After an additional 24 hours, the media was removed and frozen (-80oC freezer) for later measurement with an enzyme linked immunosorbant assay (ELISA). Cells were fixed, treated with saponin, stained with DAPI, and imaged with a confocal microscope. Images were used for cell counting and estimated the plate density.

3.12 Effect of LPS on NP Treated Cells

100,000 cells (J774A.1) were seeded on 35mm tissue culture plates with DMEM high glucose media (10% FBS, 1% anti-2). After 44 hours, a 1.2mL solution of 10% NP/Soluble DS/fddH_2O in media was administered. After 4 hours, LPS ($1mu$g/mL) in media was administered. After an additional 24 hours, the media was removed and frozen (-80^{o}C freezer) for later measurement with an enzyme linked immunosorbant assay (ELISA). Cells were fixed, treated with saponin, stained with DAPI, and imaged with a confocal microscope. Images were used for cell counting and estimated the plate density.

3.13 Statistical Analysis

Quantitative results are reported as mean SEM. Two-tailed t-tests and two-way analysis of variance ANOVA with a Bonferroni post test were utilized in determining of significance. Significance was considered with a p values ¡0.05, ¡0.01, and ¡0.001,

corresponding to single, double, and triple asterisks respectively. Experiments were performed in an independent fashion, at least in duplicate.

CHAPTER 4. RESULTS AND DISCUSSION

4.1 One-Step Nanoparticle Formation

Polyelectrolyte complex nanoparticles were fabricated with poly-L-lysine (PLL), a polycation and heparin, a polyanion under ultrasonication conditions, as shown in Figure 4.1A. Nanoparticles were initially formed with 5 minute sonication. In Figure 4.1B, varying the heparin to PLL weight ratio allowed for control of the surface charge. The surface charge mirrors the more predominant surface polymer species, therefore the surface charge can be controlled via the heparin to PLL weight ratio. For example, the 0.7 [hep]/[PLL] NP had a positive zeta potential, so PLL would be the more predominant polymer on the surface of the NP. While the charge is altered, varying the heparin/PLL weight ratio does not greatly alter the size, as shown in Figure 4.1.C and Table 4.1. Compared to reported NP size data (as shown in Table A.1), the size of these nanoparticles were smaller. This could possibly due to the molecular weight, preparation method, and concentrations of the heparin and PLL employed during fabrication. In Table B.1, the increase in heparin and PLL concentrations increased NP size. In Table A.1, the papers reporting the same molecular weights and ultrasonic conditions had a range of sizes, suggesting that the particular sonication protocol can alter NP size. Muller et al. demonstrated the size of PEC NPs composed of polyethyleneimine (PEI) and poly(acrylic acid) could be altered by adjusting the molecular weight of PEI [32]. Heparin/PLL nanoparticles may respond in a similar way.

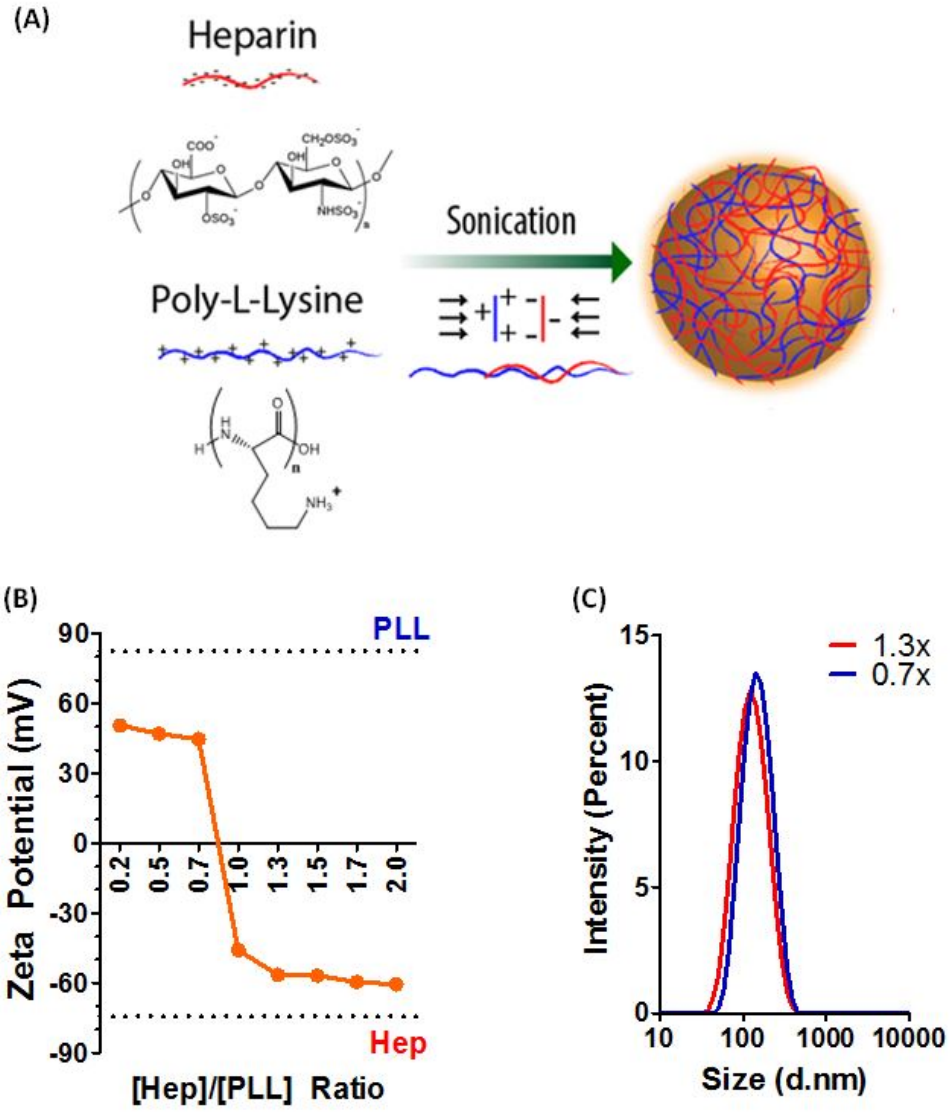

Fig. 4.1: A) Schematic representing basic nanoparticle synthesis. B) Zeta potential of NPs with varying [Hep]/[PLL] ratios at a constant [PLL] of 0.25 mg/mL. C) Representative size distribution data.

Table 4.1: Size and PDI for [Hep]/[PLL] ratios at a constant [PLL] of 0.25 mg/mL.

[Hep]/[PLL]	Size (nm)	PDI
0.2	152.1±2.6	0.172±0.022
0.5	127.0±1.3	0.208±0.023
0.7	129.5±7.4	0.166±0.007
1	114.6±4.2	0.176±0.016
1.3	126.0±6.5	0.199±0.012
1.5	123.8±5.8	0.220±0.026
1.7	119.8±4.5	0.174±0.004
2	118.9±0.4	0.173±0.012

4.2 Pulse Preparation Sonication and Two-Step Nanoparticle Formation

Polydispersity index (PDI) is a measure of particle size uniformity. PDI can influence the therapeutic performance of the NPs since the NP size can influence route of endocytosis, loading efficiency, and release rate [33,34]. To further elaborate, should the NP size distribution be large, there will be a wider range of release rates some NPs could release drug prior to reaching the intended site, thereby increasing off-targeting problems. Should the method of endocytosis affect drug delivery strategy, then a larger size distribution could have NPs not taken up by the intended route into the cell, thereby reducing the effectiveness if the secondary route is ineffective. With a goal of creating a nanoparticle system that can be repurposed for several different strategies, a lower PDI would be desired. As such, the sonication technique employed for NP fabrication was adjusted with a goal of lowering PDI. Figure 4.2.A shows three methods of sonication. Here, pulse sonication was used to represent a procedure composed of alternating sonication and cool down periods. As shown in Figure 4.2B and Table 4.2, pulse sonication (i.e., condition B) yielded NPs with significantly lower size and PDI. The additional sonication beyond the initial five minute duration likely

caused the loosely bound polymers to detach from the majority of the NPs, thereby leading to a more compact NP (Figure 4.2C).

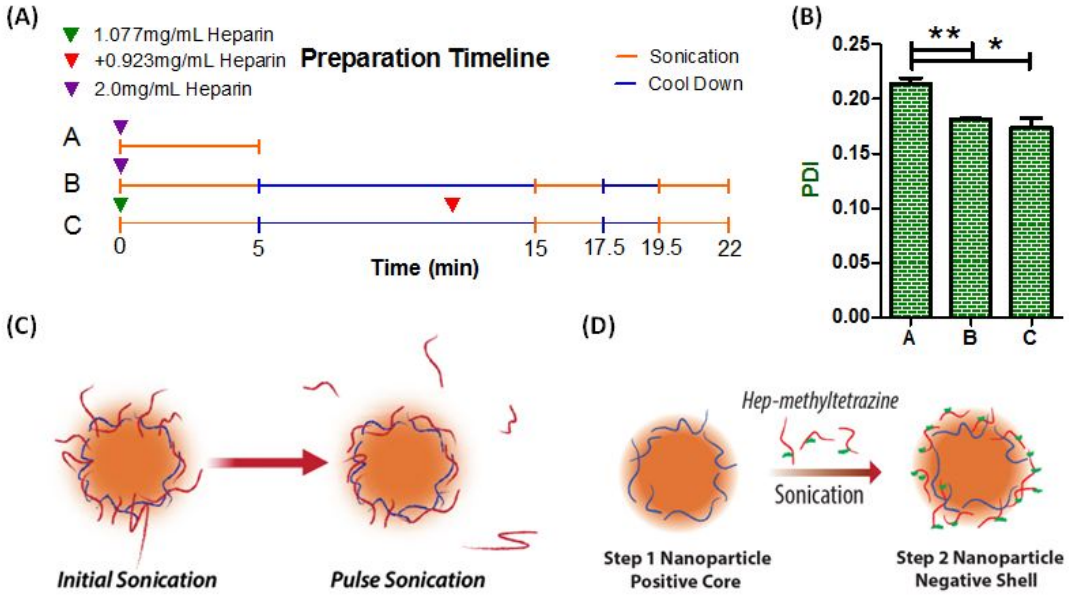

Fig. 4.2: A) Preparation timing for comparison of 1 step (A and B) and 2 step (C) method with constant overall concentrations of [Hep] 2mg/mL and [PLL] 1.538mg/mL. B) PDI results for the different preparations noted in A. C) Schematic representation of shedding loosely bound polymer. D) Schematic revealing the 2 step approach (preparation C).

Represented in Figure 4.2D, a two-step nanoparticle preparation method was developed. The two-step NP preparation method consisted of formation of a core nanoparticle with positive surface potential, followed by layering a polyanion (i.e. dextran sulfate, Tz-modified heparin, hyaluronic acid etc.). The timeline of material addition and sonication parameters employed for the two-step NP preparation method are shown as line C of Figure 4.2A. The core NP was comprised of a [Hep]/[PLL] ratio of 0.7 had a positive surface potential. The [Hep]/[PLL] ratio of 0.7 was chosen to provide adequate positive surface charges (Figure 4.1B). Upon addition of heparin, the layered NP [Hep]/[PLL] was 1.3, with a negative zeta potential (Table 4.2, preparation C). The [Hep]/[PLL] weight ratio of 1.3 was chosen due to the surface potential

(Figure 4.1B) had stabilized. In Table 4.2, comparing the NP size of preparations B and C, there is a significant increase in diameter. Considering the change in surface charge and increase diameter, the additional material was likely to be added to the surface of the NP and not reorganizing the NP completely. In Table B.2, the layering method was employed to add dextran sulfate and modified heparin onto the NP surface. Size, zeta, and PDI were similar between surface heparin and surface dextran sulfate NPs.

Table 4.2: Table of size and zeta potential for preparation timeline in Figure 4.2.

Preparation	Diameter (nm)	Zeta Potential (mV)
A	160.8±2.1	-45.5±0.8
B	144.3±1.2	-47.8±0.5
C	157.1±3.6	-46.0±0.3

4.3 Nanoparticle Stability

Shelf life, as determined by the stability of a product plays an important role for a biomedical material, since a short shelf life biomedical material will be less likely to be used. The nanoparticle stability was determined via DLS and dimethyl methylene blue (DMMB) assay over the course of a month. PDI, a measure of particle size uniformity has a scale where 0 is completely uniform and 1 in completely non-uniform. Measurements above 0.700 is considered to be too disperse for accurate DLS measurements. A large increase in PDI over sequential measurements is an indication of instability of PEC NPs. Shown in Figure 4.3A and Table 4.3A, the core nanoparticle with surface PLL (0.7 [hep]/[PLL]) had consistent size and PDI for the month of testing. Similar to the core nanoparticle, the NPs formed from two-step pulse sonication with surface heparin (1.3 [hep]/[PLL]) had consistent size and PDI

for at least a month, as seen in Figure 4.3B and Table 4.3B. The consistent size and PDI suggests the NPs are stable for at least a month.

Table 4.3: A) Size and PDI over time for 0.7 weight ratio ([PLL] 0.25 mg/mL) nanoparticles. B) Size and PDI over time for 1.3 weight ratio ([PLL] 0.25 mg/mL) nanoparticles.

(A)

Days	Diameter (nm)	PDI
0	129.5±7.4	0.166±0.007
2	128.1±8.5	0.180±0.014
6	123.5±12.0	0.206±0.019
10	119.3±14.3	0.205±0.037
17	120.4±14.2	0.215±0.028
22	121.4±14.3	0.215±0.030
29	120.4±13.3	0.214±0.030

(B)

Days	Diameter (nm)	PDI
0	119.3±0.4	0.131±0.005
2	115.5±1.6	0.153±0.013
6	114.4±2.2	0.172±0.015
8	114.0±1.9	0.170±0.016
15	113.4±1.4	0.163±0.019
22	113.4±2.4	0.161±0.016
29	114.8±2.0	0.160±0.011

In addition to size and PDI measurements, DMMB assay, a method for quantifying glycosaminoglycan content (e.g., heparin), was employed to evaluate the stability of the nanoparticles. Initial measurements of the core NP (0.7 [hep]/[PLL]) surprisingly revealed the heparin in the core was not measurable, therefore DMMB did not have access to the heparin. As such, DMMB seemed to offer another method for measuring the stability of the NPs, since a degradation of the NP would result in liberation of heparin into the solution. Within a month, there was no measurable heparin in the solution incubated with the core NP, suggesting the NP did not disintegrate and were stable for that time period. Heparin contents in the NPs formed from two-step pulse sonication were also measured via DMMB, which revealed that a portion of the total heparin was measurable. Since the PLL of the core may have masked the core heparin from detection, the DMMB measurements in the samples with NPs formed from two-step pulse sonication were indicative of heparin released to the buffer or still bound to NP surface. An increase in heparin content would signify NP disintegration. As shown in Figure 4.2.C, the heparin content in solution did not increase, suggesting the NPs are stable for at least a month, in agreement with DLS data.

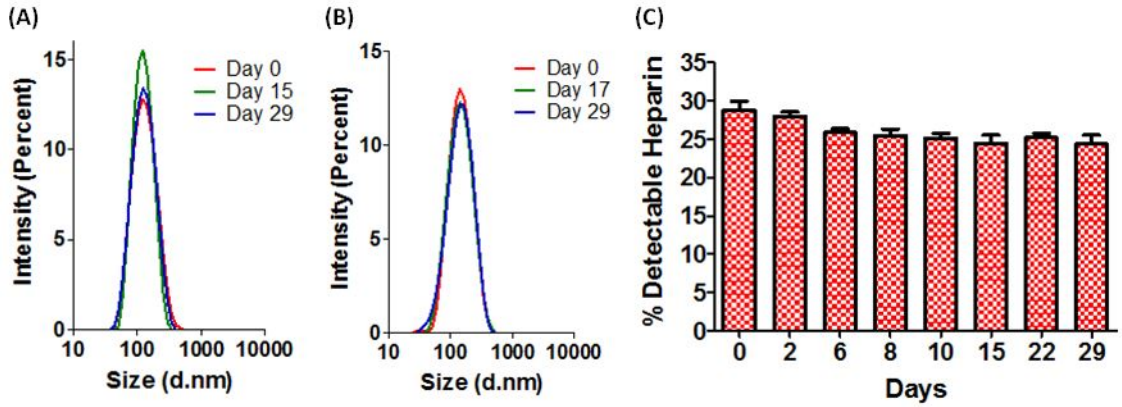

Fig. 4.3: A) Histogram overlay of 1.3 weight ratio NP size data for days 0, 15, and 29. B) Histogram overlay of 0.7 weight ratio NP size data for days 0, 17, and 29. C) Assessing stability of 1.3 weight ratio nanoparticles with [PLL] of 0.25 mg/mL using DMMB assay. Note: 0.7 weight ratio nanoparticle DMMB study was performed, but no heparin was recorded throughout the month long study.

4.4 Reaction Capabilities of Methyltetrazine Modified Heparin

Heparin was modified with tetrazine (Tz) and methyltetrazine (mTz) in order to utilize Tz:NB click chemistry for modular NP surface modification. Tz or mTz modified heparin (Tz-heparin or mTz-heparin) were synthesized via standard carbodiimide chemistry, as represented in Figure 4.4. Briefly 1-ethyl-3-(3-dimethylaminopropyl) carbodiimide (EDC) and N-Hydroxysuccunimide (NHS) were mixed with heparin to activate the carboxylic acids on heparin. The NHS-ester formed in the activated heparin will react with tetrazine-amine or methyltetrazine-amine to form amide bonds between heparin and Tz or mTz. Employing the two-step pulse sonication method, the modified heparin could be layered onto the NP surface to act as a handle for modular modification with NB-modified bioactive cues.

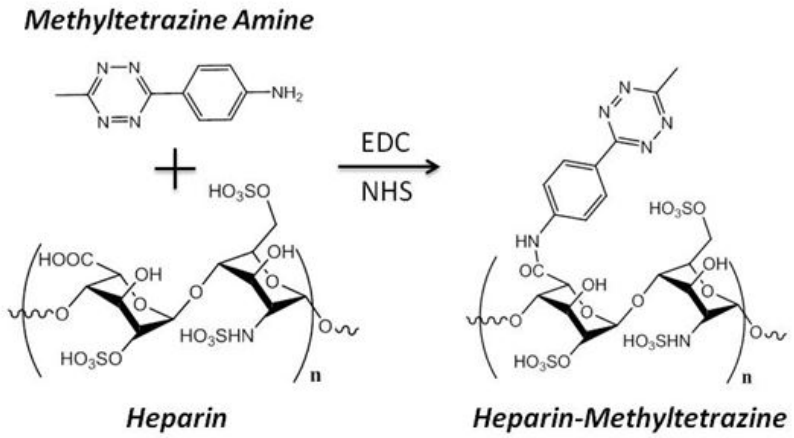

Fig. 4.4: Schematic representation of the carbodiimide crosslinker reaction with heparin and methyltetrazine amine.

The reaction kinetics of mTz-heparin and a linear methyl-PEG-NB was monitored via ^{1}H NMR. As shown in Figure 4.5A, reactions between mTz and NB moieties would result in shifting of proton peaks corresponding to the hydrogen atoms of the mTz aromatic ring (peaks A, A, B, B) and reduction NB associated protons (peaks C and D). Figure 4.5B shows an overlay of ^{1}H NMR spectra where gradual reduction of norbornene proton signals and reduction of mTz proton signals were detected for samples reacted from 0.2 to 24 hours. Figure 4.5C shows the kinetics of NB-mTz reaction. Note that there was residual norbornene proton signals left after 24 hours of reaction. This could be attributed to the amount of mTz and NB added were both based on calculations, which potentially led to more NB than mTz in solution. The inaccuracy in the actual concentration may be attributed to the heterogeneous manner of heparin, leading to less mTz used in testing than calculated. Regardless, the reaction proceeded spontaneously and was completed by about 24 hours. The reaction kinetics of Tz-NB was also attempted using the same method; however, the reaction was difficult to quantify owing to the rapid reaction rate between NB and Tz [35].

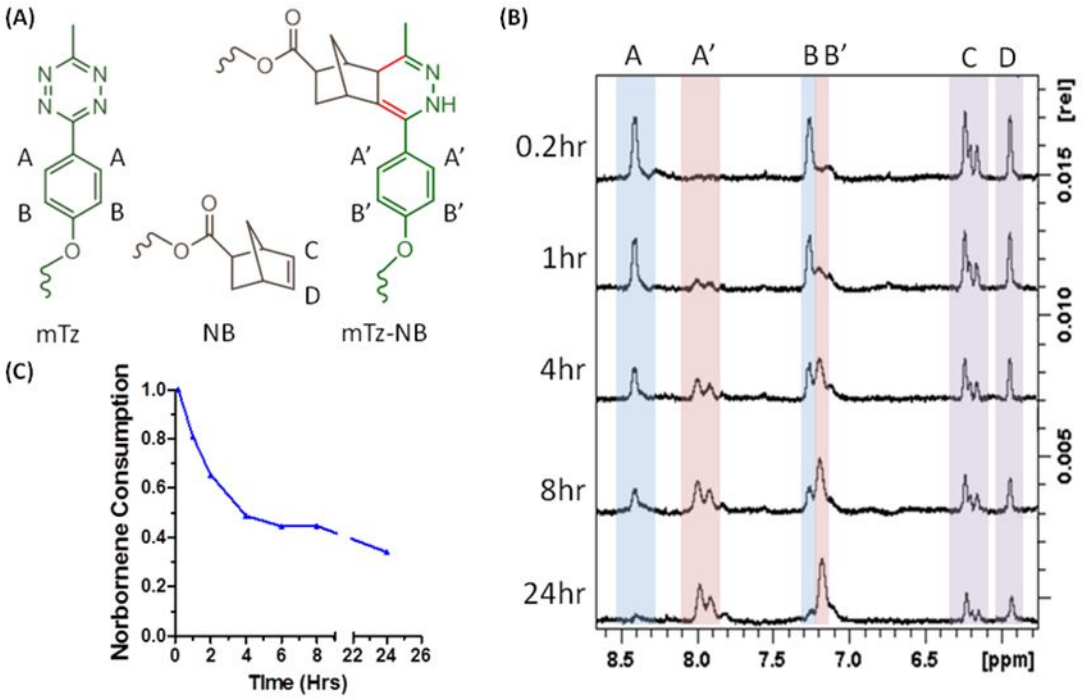

Fig. 4.5: A) Structure of methyltetrazine (mTz), Norbornene (NB), and the result of the reaction with proton labeling corresponding to peaks in Figure 4B. B) Overlay of ^{1}H NMR chromatographs of Heparin-mTz and one arm PEGNB reaction taken at specific time points. C) Graph representing NB consumption as the reaction progresses. B/B' peaks were set as a reference peak and A/A' were used as confirmation.

4.5 Reaction of Surface Tetrazine Nanoparticles with Norbornene Modified Species

To demonstrate that the NP surface tetrazine can be used for bioconjugation, a pilot study was performed for attaching norbornene-functionalized fluorescent molecules. First, two step NPs were created with Tz-heparin or mTz-heparin, as shown in Table B.2. The NP size and PDI were not greatly affected between NPs formed with Tz-heparin or mTz-heparin coating and NPs formed with heparin coating. However, a decrease in zeta potential was noted, probably due to a reduction of carboxylic

acid due to the EDC/NHS reaction. For surface conjugation, a linear Cy5-PEG-NB was synthesized by first modifying linear PEG-OH with norbornene. The resulting PEG-NB was then reacted with Cy5-Tetrazine at a Tz:NB molar ratio of 1:20. The linear Cy5-PEG-NB was employed to tag a fluorescent probe onto the NP via Tz:NB reaction, as represented in Figure 4.6A. The Cy5-PEG-NB and Tz-Hep coated NPs were simply mixed and incubated for 24 hours. Next, the NP solution was washed three times, centrifuged and resuspended in fresh ddH_2O in order to remove unreacted Cy5-PEG-NB. A droplet of this solution was imaged via confocal microscope (Figure 4.6B). The dotty red Cy5 fluorescence in the images was indicative of successful tagging of Cy5 to the surface of NPs. The Cy5-tagged NPs were also entrapped into a hydrogel for visualization. The NP-loaded hydrogels were swelled to remove unreacted soluble Cy5-PEG-NB. The NP-loaded hydrogels were imaged by confocal microscope (Figure 4.6C). Aggregation was noted and the origin was determined to be from the concentration step, since repeated studies without concentration step showed no aggregation. In Figure 4.6B and C, signal corresponding to Cy5 was present in the droplet and hydrogels. The confocal images of Figure 4.6 suggest the NB-PEG-Cy5 species was clicked onto the nanoparticles and demonstrated the Tz-heparin are on the NP surface and are available to react with norbornene modified species.

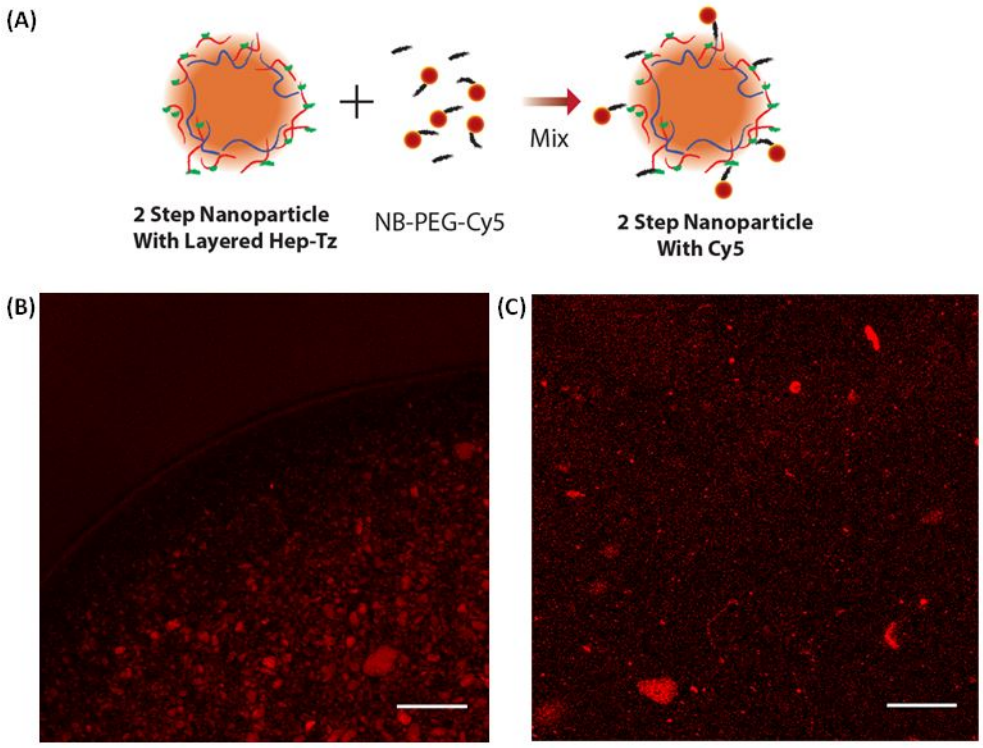

Fig. 4.6: A) Schematic representation of addition of PEG-Cy5 to the surface of the nanoparticle via tetrazine (Tz) norbornene (NB) click chemistry. Cy5 fluorescence confocal image of 2 step Cy5 NPs in the edge of a droplet (B) and in the center of a hydrogel (C). Scale 200 μm.

4.6 Cytotoxicity of Components and Nanoparticles

Cytotoxicity of NPs and their constituent polymers were determined via MTT assays on J774A.1 monocytes. In Figure 4.7A, high concentration of heparin (20mg/mL) caused slight reduction in cell viability. However, at the concentrations used for NP preparation heparin did not exhibit cytotoxic effect. As shown in Figure 4.7B, dextran sulfate was not toxic to the cells for all concentrations tested. On the contrary, poly-L-lysine was determined to be highly cytotoxic (Figure 4.7C), including at the concentration in NP fabrication (0.25mg/mL). Considering the cytotoxic effect of PLL, it was critical to evaluate the cytotoxicity of nanoparticles. As shown in Figure

4.7D, the NP cytotoxicity assay was performed with equal concentrations of PLL for NP and soluble PLL groups. In spite of the use of a soluble PLL concentration that would have cause cell death, NPs formed at this PLL concentration actually promoted cell proliferation as more than 100% of MTT signals were obtained from these samples when compared with the control group. It was possible that these NPs, which were heparinized on the surface, sequestered more serum proteins and resulted in increased uptake by the cells. Consequently, forming NPs with surface heparin not only reduced the cytotoxicity of PLL, but also exerted an unexpected effect on promoting cell proliferation.

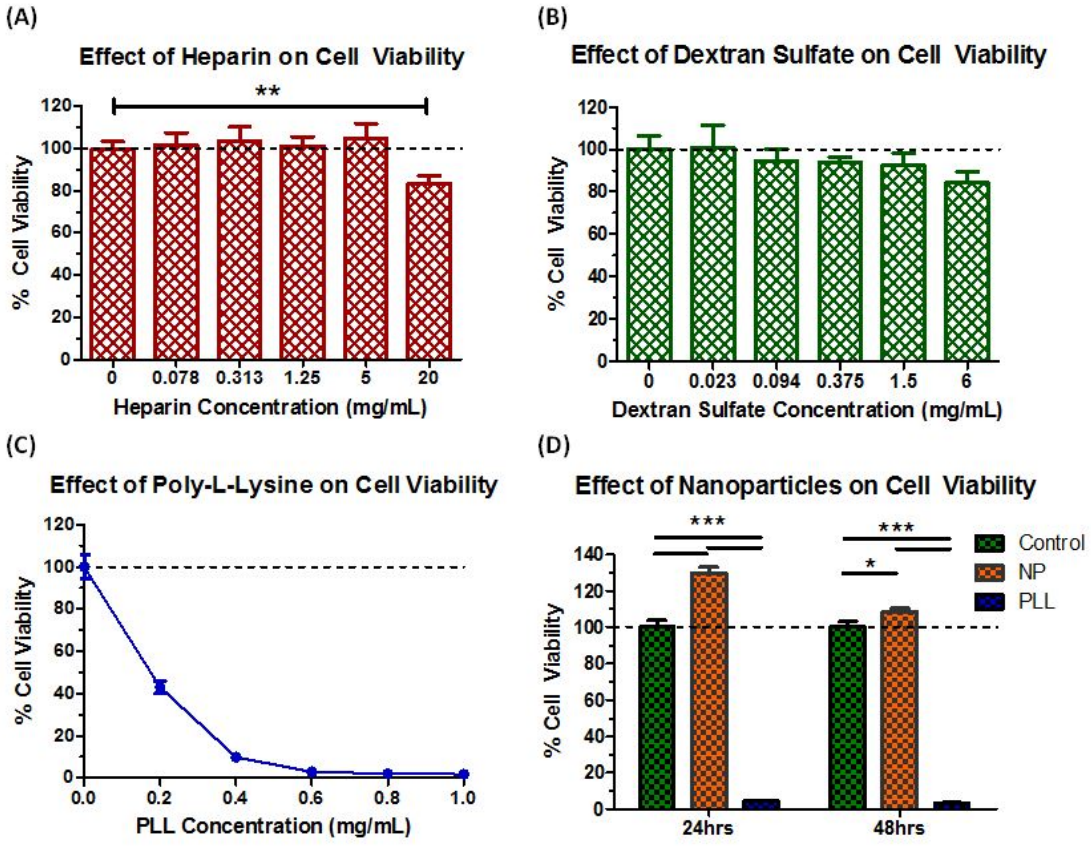

Fig. 4.7: MTT assay determining cell viability of J774A.1 monocyte cells with 4hrs of incubation with nanoparticle components. Components are: A) heparin, B) dextran sulfate, and C) poly-L-lysine. D) MTT assay determining J774A.1 cell viability with 24 and 48 hour incubation with 2 step heparin surface nanoparticles.

4.7 Modulation of Nanoparticle Recognition/Uptake by J774A.1 Monocytes, Macrophages, and 3T3 Fibroblasts

Modulation of cellular uptake/recognition of NP is important for targeted delivery of therapeutics to cells. When delivered into the body, NPs can be cleared by macrophages, which is problematic for therapeutic applications of nanoparticle. Strategies to increase NP circulation time are therefore important as they can increase the amount of drug getting to the desired location. Modulating uptake/recognition could also increase interaction of a nanoparticle with a specific cell type for treatment. As such, an investigation into the uptake modulation capabilities of the NPs formed by two-step pulse sonication was undertaken. NPs formed by two-step pulse sonication were prepared with dextran sulfate, heparin, or Tz-heparin coating (Table B.2). Tz-heparin NPs were used as they can be PEGylated (through reacting with linear PEG-NB). The PEG polymer chains can 'shield' the NP from macrophages, thereby improving circulation time. The studies were performed on naive (non-LPS treated) and LPS-activated J774A.1 cells. Monocytes (e.g., nave J774A.1) and macrophages (e.g., LPS-activated J774A.1) are both immune cells that are likely to come in contact with NPs. A non-immune cell type, NIH/3T3 fibroblast was used as a non-target cell type. To visualize NP uptake by the cells, PLL was first fluorescently labeled with 5(6)-carboxyfluorescene (5(6)-Fam) prior to incorporating into the NPs. In the first study, the ability of the NPs to modulate cellular uptake/recognition by LPS-activated macrophages was evaluated. Since macrophages are in tissue, this cell type is likely to come in contact with NPs, potentially close to the site of treatment. As such, the NPs were administered to LPS activated J774A.1 macrophages, which exhibited an M1 phenotype [37-39]. In 5(6)-Fam column of Figure 4.8A, there is a clear decrease in fluorescence between heparin-coated NP and PEGylated NP groups. The cell nuclei were counter-stained with DAPI for cell counting, while differential interference contrast (DIC) images were obtained to show cell morphology. The spread cell morphology of a large portion of the cell population confirmed the LPS activation of

the J774A.1 monocytes. Figure 4.8B shows the results of image analysis where fluorescent intensity was normalized to cell number. Clearly, PEGylation of NP decreased cellular uptake, which is in agreement with previously reported literature [18, 20–23]. Furthermore, comparing NPs coated with Tz-heparin and with heparin, there was no significant difference in the amount of NP uptake by the cells. Therefore, it can be concluded that the surface tetrazine was not responsible for the decrease in cellular uptake for the PEGylated group.

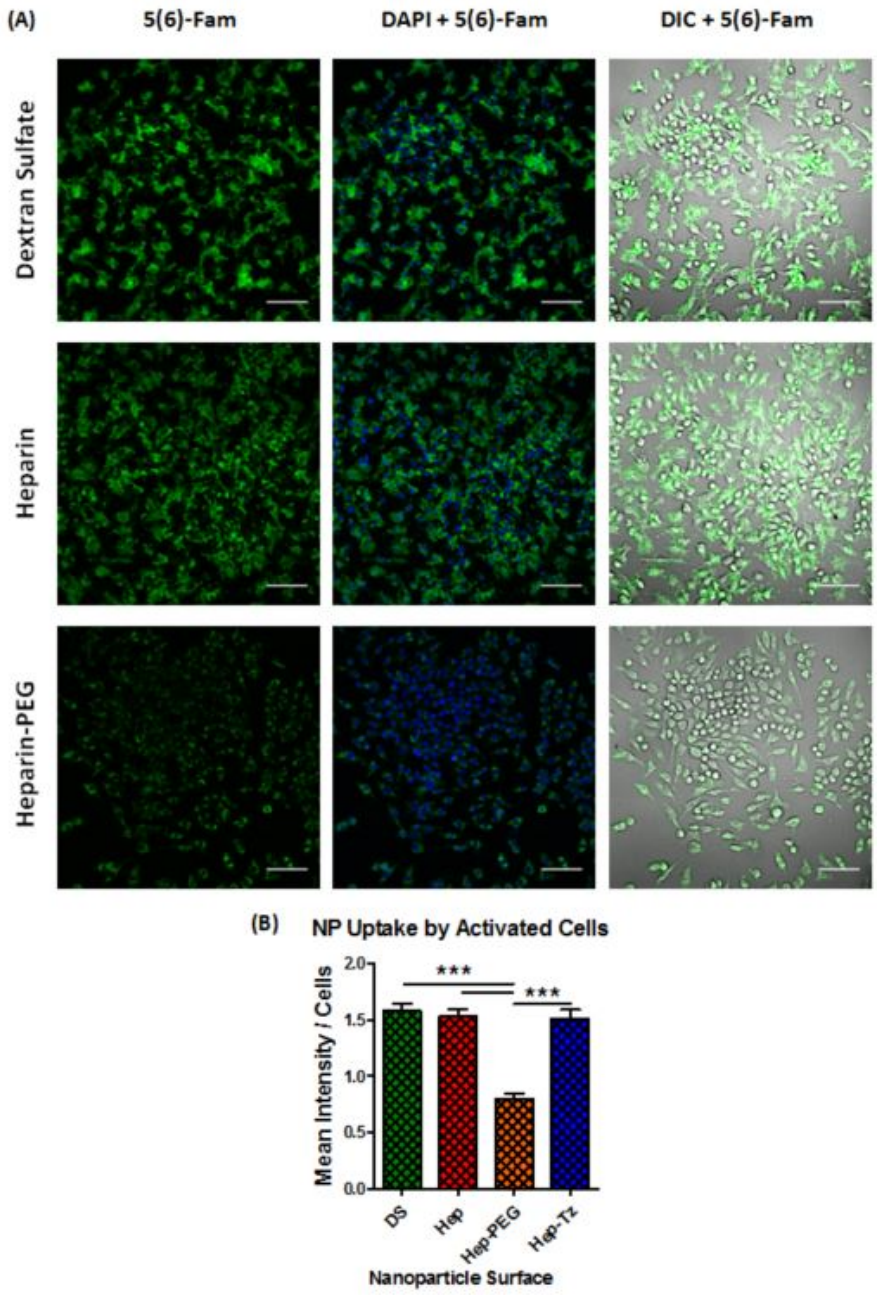

Fig. 4.8: A) Nanoparticle uptake by LPS activated J77A.1 cells after four hours of treatment. NPs had surface of either dextran sulfate, heparin, or heparin-Tz conjugated with linear PEG-NB. Nanoparticles were modified with 5(6) carboxy fluorescene for imaging purposes. Scale 100μm. B) Intensity of 5(6)-fam per cell were determined for images of LPS activated J774A.1 cells with corresponding surfaces. (approximately 300 cells per image).

In the second study, the ability of the NPs to modulate cellular uptake/recognition by monocytes was evaluated. Since monocytes are in blood, NPs are almost certain to come in contact with this cell type. In 5(6)-Fam column of Figure 4.9A, again there is a clear decrease in fluorescence between heparin coated NP and PEGylated NP groups. The morphology of the cells treated with PEGylated NPs were more circular, suggesting that the cells remained as nave monocytes. However, there was more spreading in the cells treated with either dextran sulfate or heparin coated nanoparticles, suggesting that the cells could have been activated due to the uptake of NPs. Figure 4.9B shows the results of image analysis where fluorescent intensity was normalized to cell number. Again, PEGylation of the NPs decreased cellular uptake, similar to that observed in the experiment with LPS-activated J774A.1 macrophages.

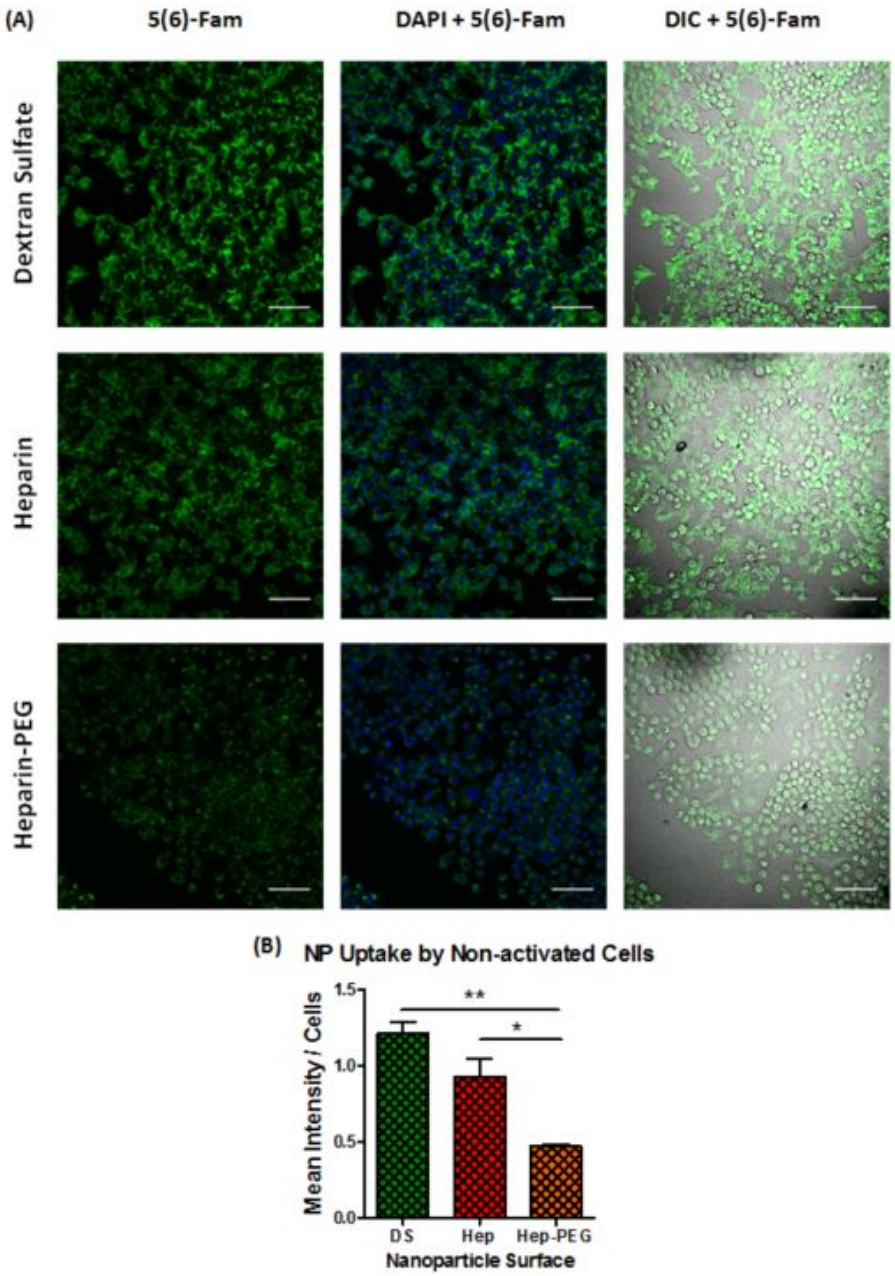

Fig. 4.9: A) Nanoparticle uptake by non-activated J77A.1 cells after four hours of treatment. NPs had surface of either dextran sulfate, heparin, or heparin-Tz conjugated with linear PEG-NB. Nanoparticles were modified with 5(6) carboxy fluorescene for imaging purposes. Scale 100μm. B) Intensity of 5(6)-fam per cell were determined for images of non-activated J774A.1 cells with corresponding surfaces. (approximately 500 cells per image).

In the third study, the ability of the NPs to modulate cellular uptake/recognition by non-immune cells was evaluated. Off target binding to cells not intended for treatment can be problematic for therapeutic applications. Therefore, a study was performed to evaluate whether NP surface modification altered uptake/recognition by non-immune cells. In 5(6)-Fam column of Figure 4.10A, there is a clear decrease in fluorescence between heparin coated NP and PEGylated NP groups as well as between heparin coated NP and dextran sulfate coated NPs. Figure 4.10B shows the results of image analysis where fluorescent intensity was normalized to cell number. Clearly, PEGylation of NP decreased cellular uptake, which agrees with previous data. Dextran sulfate coated NPs also clearly decreased cellular uptake. In the previously shown data, dextran sulfate coating did not change uptake by monocytes/macrophages. As a component of the ECM, heparin likely interacts with fibroblast cells. As product of gram negative bacteria, dextran sulfate probably does not regularly interact with fibroblast cells. Therefore, a reduction of recognition from NP surface heparin to surface dextran sulfate is not surprising.

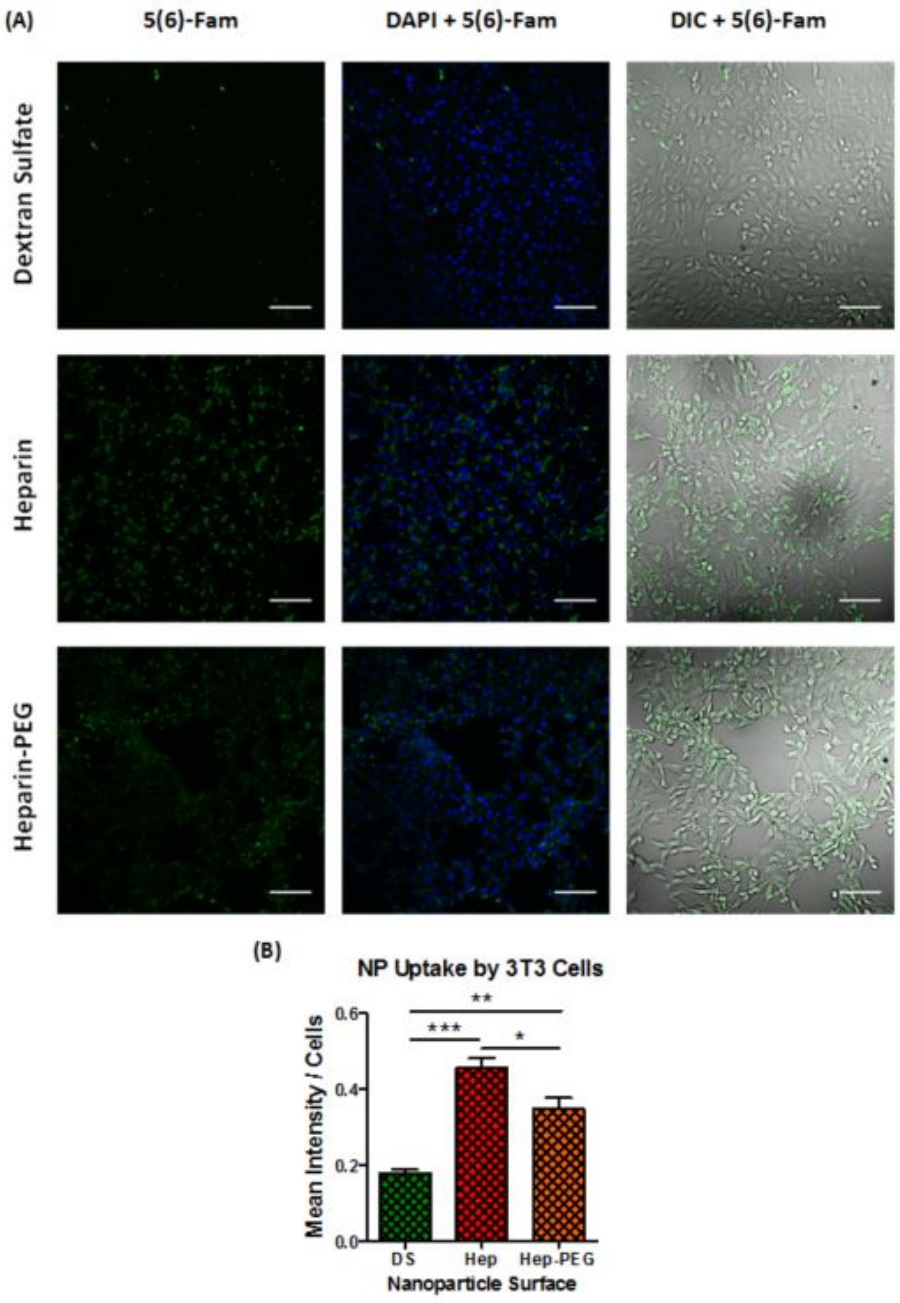

Fig. 4.10: A) Nanoparticle recognition/uptake by 3T3 cells after four hours of treatment. NPs were coated with either dextran sulfate, heparin, or heparin-Tz conjugated with linear PEG-NB. Nanoparticles were modified with 5(6) carboxy fluorescene for imaging purposes. Scale 100μm. B) Intensity of 5(6)-fam per cell were determined for images of 3T3 cells with corresponding surfaces. (approximately 500 cells per image).

The ability to selectively target a specific cell type reduces off targeting effects, making for a more effective therapeutic carrier. Therefore, NP uptake by different cells were compared. As shown in Figure 4.11, J774A.1 cells clearly uptake more NPs than 3T3 fibroblasts, regardless of NP formulations. This revelation was expected due to the nature of the J774A.1 monocytes/macrophages, tasked with clearance of foreign entities. Figure 4.11 also shows that dextran sulfate coating can be employed to aid in selective cell targeting. Dextran sulfate may be selective due to macrophage scavenger receptor A recognizes and mediates endocytosis of dextran sulfate [36, 37]. Macrophages are responsible for elimination of foreign mater and production of pro or anti-inflammatory cytokines. As such, a macrophage targeting platform would prove to be beneficial for disease treatment. Macrophages in inflammatory diseases are activated to the M1 phenotype, producing pro-inflammatory cytokines and reducing the ability for the area to heal. Reduction of the M1 population or repolarize M1 macrophage to the anti-inflammatory M2 macrophage could aid in recovery of arthritic tissue. As such, the ability to selectively target macrophage for inflammatory disease treatment is very beneficial. The selective cell targeting by dextran sulfate also suggests the NPs formed from two-step pulse sonication can employ layering a variety of polyanions for modifying how the NPs interact with cells.

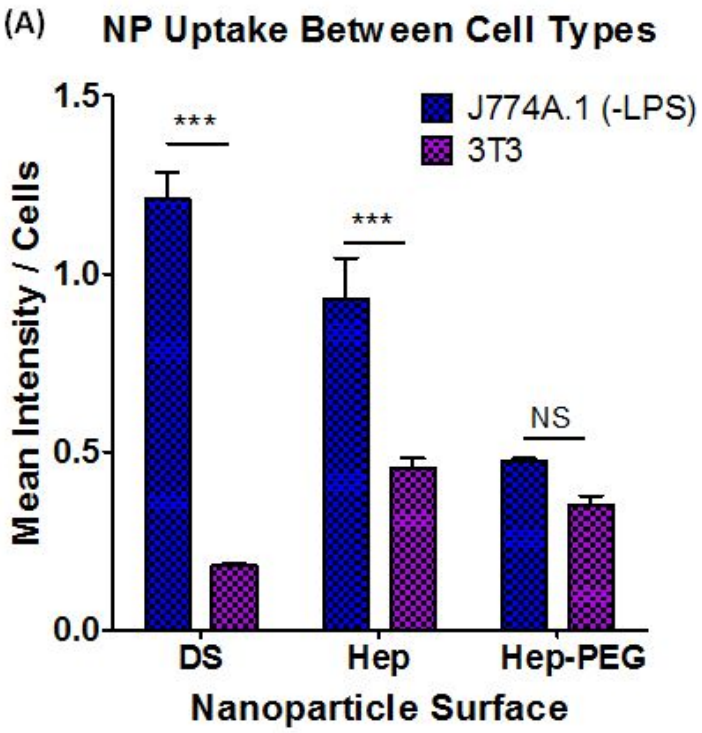

Fig. 4.11: A) Comparison of cellular uptake with similar cell density (approximately 500 cells per image).

4.8 RGD-Bound Nanoparticle Recognition by 3T3 Fibroblast Cells

To further demonstrate the ability of the NPs formed from two-step pulse sonication to modulate cellular recognition, an integrin binding peptide was affixed to the surface of the NPs. As a trans-membrane receptor, integrin facilitates cell adhesion to the ECM. Attaching RGD to a NP surface has been employed as a method for increasing colocalization of NPs to a cells surface for disease treatment, such as a breast cancer with an over expression of integrins [38]. A model GGGRGDS peptide, which contains the integrin binding sequence RGD, was modified with norbornene via HATU coupling reaction. Briefly, 5-norbornene-2-carboxylic acid and HATU were mixed to activate the carboxylic acid group. Purified GGGRGDS was then added to the acti-

vated norbornene solution. The peptide N-terminal primary amine reacted with the activated carboxylic acid to yield a norbornene-modified RGDS peptide. The NB-GGGRGDS peptide was affixed to heparin-Tz coated NPs via Tz:NB click reaction. NPs with and without the RGD peptide were administered to 3T3 fibroblasts. As shown in Figure 4.12, the control NPs (no RGDS sequence) and RGDS modified NPs were equally distributed throughout the cells. RGD peptide sequence has been shown to bind to several different integrins [39]. As such, this result was not expected, going against previous research data demonstrating the use of NP surface RGD to improve cellular localization [38, 40]. The deviation from previous data may be due to heparin exhibiting non-specific binding to fibroblast cells, masking the effect of the NP modification. As such, future testing could use a bio-inert polyanion, such as alginate to modify with RGD peptide sequence. Without non-specific binding to the cells, RGD modification of alginate coated NPs should be able to modulate cellular localization.

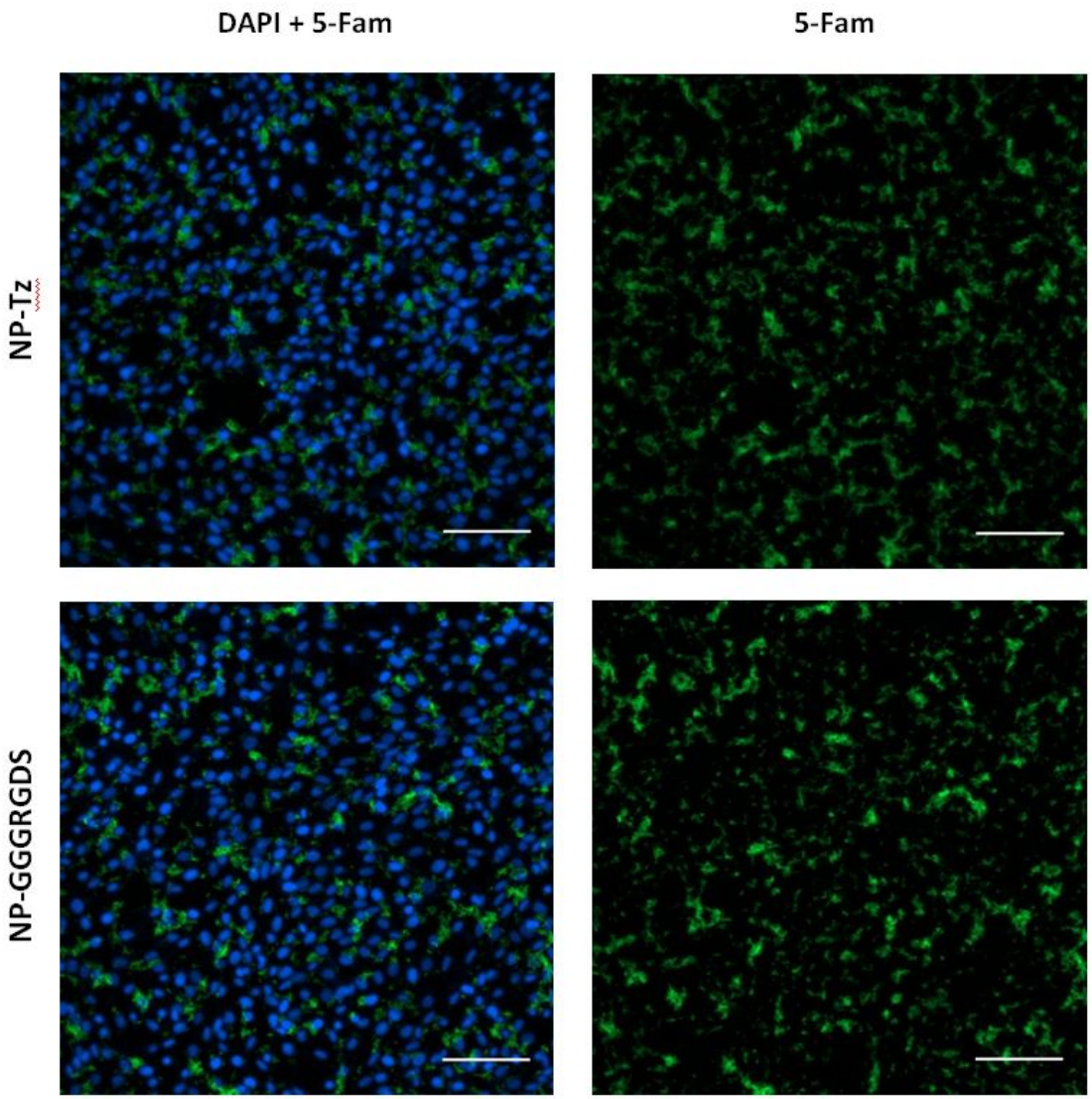

Fig. 4.12: Images of NP recognition by fibroblast (3T3) cells. NPs were coated with either heparin or heparin-Tz conjugated with NB-GGGRGDS. Cells were treated with nanoparticles for four hours. Nanoparticles were modified with 5(6) carboxy fluorescene for imaging purposes. 100,000 cells were seeded and cultured three days prior to NP treatment. Scale 100μm.

4.9 Tuning J774A.1 Macrophage Activation

To demonstrate the ability of the nanoparticles to modify macrophages, IL-10 secretion was measured from LPS activated macrophages. Two studies were performed to evaluate whether NPs could mitigate LPS mediated activation or prevent activation of macrophages by LPS. LPS classically activates J774A.1 monocytes to M1 macrophages and moderately increases IL-10 production [41]. On the other hand, IL-10 production for M2 macrophages would be greatly increased [42]. In both studies, IL-10 production was measured with ELISA. In order to understand production on a per cell basis, cell nuclei were counter-stained with DAPI and counted from confocal images.

The first study was performed to evaluate whether NPs could mitigate LPS mediated activation. The ability to repolarize or reduce further activation could be beneficial for treating inflammatory diseases, since repolarization or a reduction of M1 macrophages should reduce pro-inflammatory cytokines. The reduction of pro-inflammatory cytokines should reduce inflammation which would be beneficial for healing the inflammation site. As such, cells were initially activated by LPS, followed by administration of either soluble dextran sulfate, dextran sulfate-coated NPs, or no materials. Exact treatment times are shown in the timeline in Figure 4.13A. At the time aliquots were taken, each group had similar cell densities, suggesting soluble DS and DS-coated NPs did not have an effect on cell proliferation when treated after activation. Soluble dextran sulfate significantly decreased IL-10 concentration/production both on the basis of concentration (Figure 4.13B) and cell count (Figure 4.13C)). Administration of NPs caused a moderate, but not statistically significant, decrease in IL-10 production. As such, soluble DS seemed capable of shifting phenotype activation, while the nanoparticles cannot. These results were different from that reported in the literature. For example, Kono et al. demonstrated soluble dextran sulfate decrease IL-12 production while increasing IL-10 production of mouse peritoneal macrophages [43]. In addition to the difference in cell sources, it

was likely that the timing of material addition and the concentration of LPS used to activate macrophage were different. Specifically, Kono et al. activated macrophages with 10 ng/mL LPS at the same time as dextran sulfate administration, while this study activated macrophages with 1 μg/mL LPS for 24 hours prior to administration of dextran sulfate or dextran sulfate coated NPs. While further studies are required to clarify the influence of dextran sulfate (soluble or NP form) on activated macrophages, this study has demonstrated that the DS coated NPs were potentially capable of shifting macrophage phenotype.

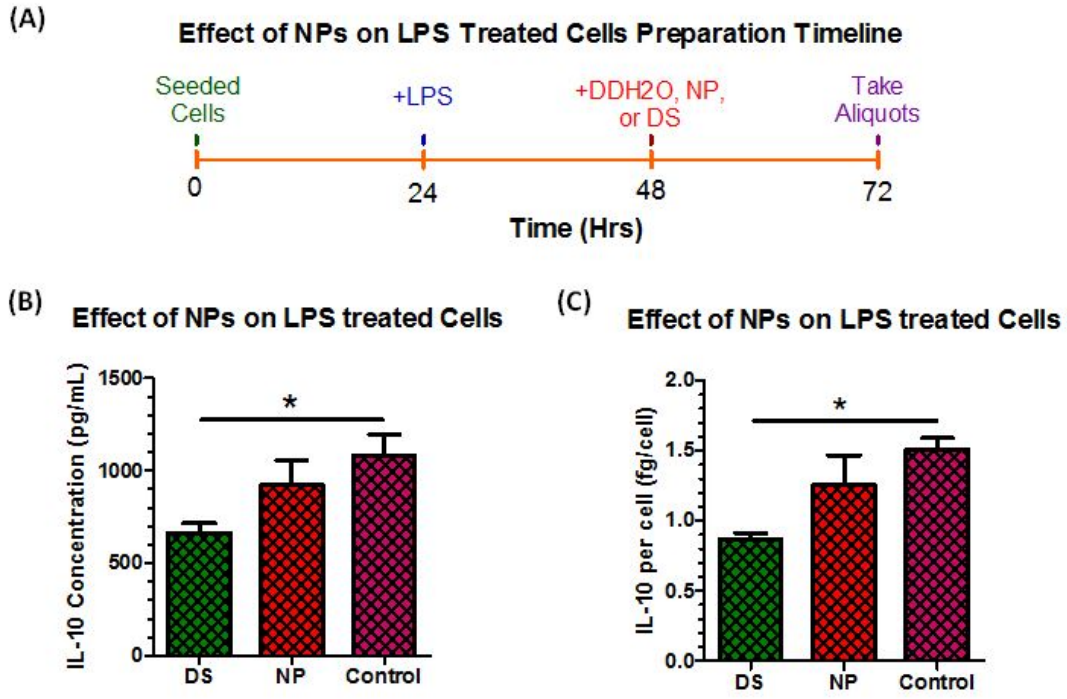

Fig. 4.13: A) Treatment timeline for testing the effect of NPs on LPS treated cells. B) Measurement of IL-10 production from cells treated with LPS followed by NPs (n=5). C) Measurement of IL-10 production per cell, from cells treated with LPS followed by NPs (n=5).

To evaluate whether the NPs could prevent activation of macrophage by LPS, a second study was performed on cells treated with first NPs followed by LPS. Prevent-

ing activation could be useful in situations where a medical procedure could induce unwanted macrophage activation, such as administrion of a stent. As such, cells were initially treated with either no materials, soluble dextran sulfate, or dextran sulfate coated NPs for four hours. From NP uptake studies performed earlier, four hours was adequate for NP uptake by naive J774A.1 monocytes. Figure 4.14A outlines the experimental timeline. As shown in Figure 4.14B, soluble DS treatment led to slight increase in IL-10 concentration/production. When IL-10 production was normalized to cell count (Figure 4.14C), DS-coated NPs decreased IL-10 production on a per cell basis. However, there was no statistical significance in the difference between all three groups. Cells were seeded at the same density, however the density after treatment was higher for both soluble DS and DS coated NPs (Figure 4.14C). The increased cell density suggests NPs promoted proliferation. The decrease in IL-10 production for DS coated NP group suggests that there is possibly an inhibitory effect of the NPs to LPS activation. Additional experiments are required to elucidate whether the DS coated NPs decrease macrophage activation by LPS.

As stated previously, the NP treatment time of the second study on macrophage activation was 4 hours, as opposed to the 24 hour treatment of the the first study. The four hour time was adequate to have considerable uptake by DS coated NPs, while the short timeframe may have been inadequate for soluble DS uptake. Therefore the NPs likely facilitated DS uptake by macrophages, allowing for a larger amount a DS to be uptaken in a shorter time (Figure C.1). A 24 hour treatment time for soluble DS could possibly lead to more uptake and a similar inhibition of macrophage activation. Nonetheless, further testing are required to examine this hypothesis.

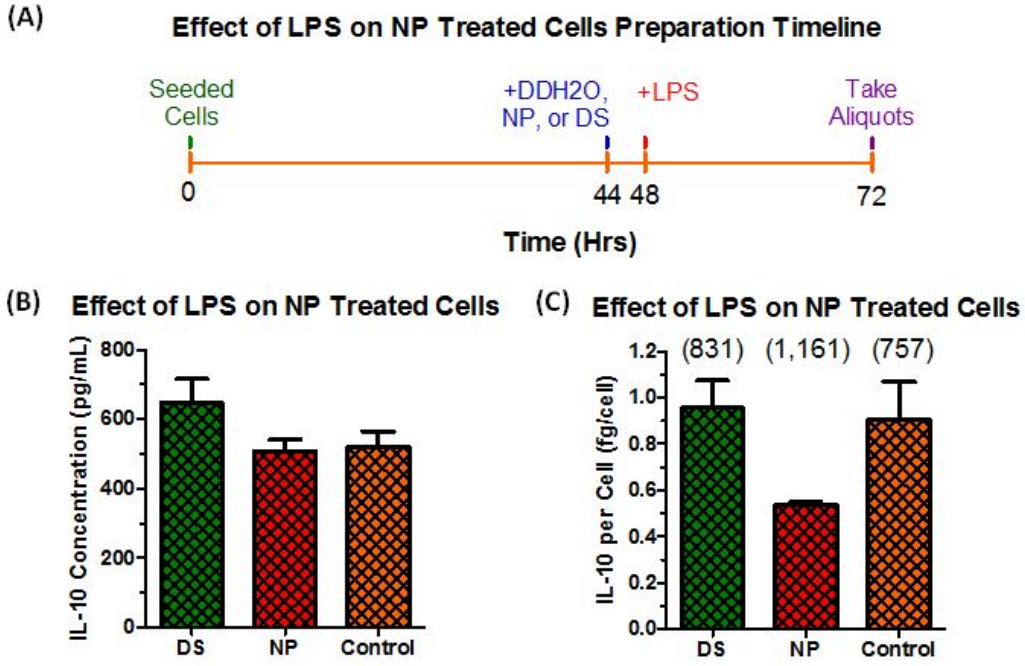

Fig. 4.14: A) Treatment timeline for testing the effect of LPS on NP treated cells. B) Measurement of IL-10 production from cells treated with NPs followed by LPS (n=4). C) Measurement of IL-10 production per cell, from cells treated with NPs followed by LPS (n=4) (p=0.063 NP DS v DS). Cell count per plate (in thousands) above respective group.

CHAPTER 5. SUMMARY & RECOMMENDATIONS

5.1 Summary

In summary, a modular nanoparticle system was developed to provide tunable surface modification and selective cell targeting. Specifically, a pulse sonication protocol was established for forming core-shell heparin/PLL nanoparticles whose surface could be modularly coated with heparin, (m)Tz-heparin, or dextran sulfate. Uniquely, the introduction of (m)Tz motif on nanoparticle surface permitted facile conjugation of inert polymer or bioactive ligand via norbornene-tetrazine click reaction. To demonstrate the modularity of NP surface modification, nanoparticles were PEGylated to reduce macrophage uptake. On the other hand, a cell adhesive peptide RGDS was clicked to the NP surface to enhance cellular uptake and recognition. Furthermore, coating NP surface with dextran sulfate effectively altered the cellular selectivity of the NP and cytokine production. Overall, this work demonstrates the versatility of the modular NP system.

5.2 Recommendations

The study designed to determine whether nanoparticles could prevent activation of macrophages did not clarify whether dextran sulfate-coated NPs inhibited LPS activation of macrophages. Thus, future studies with adjustments to the testing parameters are recommended. Additionally, testing secretion of other cytokines, such as IL-6, IL-12, or TNF-α, should be measured to compliment the finding from the IL-10 production. NP uptake was suspected to be the cause of the difference between the

moderate inhibitory effect of the DS-coated NPs and the soluble DS. Thus, a 24-hour pretreatment with NPs and soluble DS should provide clarity on whether soluble DS will act in a similar fashion. Another method to clarify the cause of the difference in activation inhibition will be to compare uptake capabilities of fluorescent-labeled DS and fluorescent DS-coated NPs.

Modulating cell localization of NPs with RGDS surface modification was not successful, possibly due to non-specific binding of heparin to the fibroblast cell surface. As such, the use of a bio-inert polyanion, could reduce non-specific binding, allowing for modulation of cell localization with RGDS surface modification.

Even though NPs prepped by two-step pulse sonication demonstrated easy modification, the Tz-heparin coated NPs were not used for a specific application. Future studies can delve into using NPs as biomarkers or drug carriers. The ease of modification should allow for tagging NPs with a variety of antibodies, for labeling and for targeted delivery to a variety of cell types.

Finally, future studies may utilize heparin's ability to bind to proteins, enzymes, or growth factors. This material characteristic should be beneficial for sequestration and sustained release of growth factors for promoting tissue regeneration.

LIST OF REFERENCES

LIST OF REFERENCES

[1] C. C. You, O. R. Miranda, B. Gider, P. S. Ghosh, I. B. Kim, B. Erdogan, S. A. Krovi, U. H. Bunz, and V. M. Rotello, "Detection and identification of proteins using nanoparticle-fluorescent polymer 'chemical nose' sensors," *Nat Nanotechnol*, vol. 2, no. 5, pp. 318–23, 2007. [Online]. Available: https://www.ncbi.nlm.nih.gov/pubmed/18654291

[2] S. Lu, V. B. Morris, and V. Labhasetwar, "Effectiveness of sirna delivery via arginine-rich pei-based polyplex in metastatic and doxorubicin resistant breast cancer cells," *Journal of Pharmacology and Experimental Therapeutics*, vol. 369, no. 2, 2019. [Online]. Available: http://jpet.aspetjournals.org/content/early/2019/04/02/jpet.119.256909

[3] H. Nosrati, P. Barzegari, H. Danafar, and H. Kheiri Manjili, "Biotin-functionalized copolymeric peg-pcl micelles for in vivo tumour-targeted delivery of artemisinin," *Artif Cells Nanomed Biotechnol*, vol. 47, no. 1, pp. 104–114, 2019. [Online]. Available: https://www.ncbi.nlm.nih.gov/pubmed/30663422

[4] E. Vuorimaa-Laukkanen, E. S. Lisitsyna, T. M. Ketola, E. Morin-Pickardat, H. Liang, M. Hanzlikova, and M. Yliperttula, "Difference in the core-shell dynamics of polyethyleneimine and poly(l-lysine) dna polyplexes," *Eur J Pharm Sci*, vol. 103, pp. 122–127, 2017. [Online]. Available: https://www.ncbi.nlm.nih.gov/pubmed/28330769

[5] G. X. Zhao, H. Tanaka, C. W. Kim, K. Li, D. Funamoto, T. Nobori, Y. Nakamura, T. Niidome, A. Kishimura, T. Mori, and Y. Katayama, "Histidinylated poly-l-lysine-based vectors for cancer-specific gene expression via enhancing the endosomal escape," *J Biomater Sci Polym Ed*, vol. 25, no. 5, pp. 519–34, 2014. [Online]. Available: https://www.ncbi.nlm.nih.gov/pubmed/24460548

[6] S. E. Sakiyama-Elbert, "Incorporation of heparin into biomaterials," *Acta Biomater*, vol. 10, no. 4, pp. 1581–7, 2014. [Online]. Available: https://www.ncbi.nlm.nih.gov/pubmed/24021232

[7] T. Kim, J. E. Lemaster, F. Chen, J. Li, and J. V. Jokerst, "Photoacoustic imaging of human mesenchymal stem cells labeled with prussian blue-poly(l-lysine) nanocomplexes," *ACS Nano*, vol. 11, no. 9, pp. 9022–9032, 2017. [Online]. Available: https://www.ncbi.nlm.nih.gov/pubmed/28759195

[8] J. Jiang, Y. Chen, Y. Zhu, X. Yao, and J. Qi, "Efficient in vitro labeling of human prostate cancer cells with superparamagnetic iron oxide nanoparticles," *Cancer Biother Radiopharm*, vol. 26, no. 4, pp. 461–7, 2011. [Online]. Available: https://www.ncbi.nlm.nih.gov/pubmed/21812654

[9] M. S. Kang, K. H. Son, T. H. Lee, S. M. Chang, S. W. Han, and H. K. Shin, "Development of chemically signal amplified nano-biosensor mediated by poly-l-lysine," *J Nanosci Nanotechnol*, vol. 19, no. 3, pp. 1786–1789, 2019. [Online]. Available: https://www.ncbi.nlm.nih.gov/pubmed/30469267

[10] M. S. Niepel, B. K. Ekambaram, C. E. H. Schmelzer, and T. Groth, "Polyelectrolyte multilayers of poly (l-lysine) and hyaluronic acid on nanostructured surfaces affect stem cell response," *Nanoscale*, vol. 11, no. 6, pp. 2878–2891, 2019. [Online]. Available: https://www.ncbi.nlm.nih.gov/pubmed/30688341

[11] T. Liu, Y. Liu, Y. Chen, S. Liu, M. F. Maitz, X. Wang, K. Zhang, J. Wang, Y. Wang, J. Chen, and N. Huang, "Immobilization of heparin/poly-(l)-lysine nanoparticles on dopamine-coated surface to create a heparin density gradient for selective direction of platelet and vascular cells behavior," *Acta Biomater*, vol. 10, no. 5, pp. 1940–54, 2014. [Online]. Available: https://www.ncbi.nlm.nih.gov/pubmed/24342042

[12] K. Na, S. Kim, K. Park, K. Kim, D. G. Woo, I. C. Kwon, H. M. Chung, and K. H. Park, "Heparin/poly(l-lysine) nanoparticle-coated polymeric microspheres for stem-cell therapy," *J Am Chem Soc*, vol. 129, no. 18, pp. 5788–9, 2007. [Online]. Available: https://www.ncbi.nlm.nih.gov/pubmed/17428050

[13] T. Liu, Y. Hu, J. Tan, S. Liu, J. Chen, X. Guo, C. Pan, and X. Li, "Surface biomimetic modification with laminin-loaded heparin/poly-l-lysine nanoparticles for improving the biocompatibility," *Mater Sci Eng C Mater Biol Appl*, vol. 71, pp. 929–936, 2017. [Online]. Available: https://www.ncbi.nlm.nih.gov/pubmed/27987790

[14] L. Zhang, Y. Zhou, G. Li, Y. Zhao, X. Gu, and Y. Yang, "Nanoparticle mediated controlled delivery of dual growth factors," *Sci China Life Sci*, vol. 57, no. 2, pp. 256–62, 2014. [Online]. Available: https://www.ncbi.nlm.nih.gov/pubmed/24430559

[15] Y. Liu, J. Zhang, J. Wang, Y. Wang, Z. Zeng, T. Liu, J. Chen, and N. Huang, "Tailoring of the dopamine coated surface with vegf loaded heparin/poly-l-lysine particles for anticoagulation and accelerate in situ endothelialization," *J Biomed Mater Res A*, vol. 103, no. 6, pp. 2024–34, 2015. [Online]. Available: https://www.ncbi.nlm.nih.gov/pubmed/25256819

[16] T. Liu, Z. Zeng, Y. Liu, J. Wang, M. F. Maitz, Y. Wang, S. Liu, J. Chen, and N. Huang, "Surface modification with dopamine and heparin/poly-l-lysine nanoparticles provides a favorable release behavior for the healing of vascular stent lesions," *ACS Appl Mater Interfaces*, vol. 6, no. 11, pp. 8729–43, 2014. [Online]. Available: https://www.ncbi.nlm.nih.gov/pubmed/24731022

[17] C. Chen, S. Li, K. Liu, G. Ma, and X. Yan, "Co-assembly of heparin and polypeptide hybrid nanoparticles for biomimetic delivery and anti-thrombus therapy," *Small*, vol. 12, no. 34, pp. 4719–25, 2016. [Online]. Available: https://www.ncbi.nlm.nih.gov/pubmed/27043722

[18] D. Bamberger, D. Hobernik, M. Konhauser, M. Bros, and P. R. Wich, "Surface modification of polysaccharide-based nanoparticles with peg and dextran and the effects on immune cell binding and stimulatory characteristics," *Mol Pharm*, vol. 14, no. 12, pp. 4403–4416, 2017. [Online]. Available: https://www.ncbi.nlm.nih.gov/pubmed/29063757

[19] Y. Matsumura, Y. Enomoto, M. Takahashi, and S. Maenosono, "Metal (au, pt) nanoparticle-latex nanocomposites as probes for immunochromatographic test strips with enhanced sensitivity," *ACS Appl Mater Interfaces*, vol. 10, no. 38, pp. 31 977–31 987, 2018. [Online]. Available: https://www.ncbi.nlm.nih.gov/pubmed/30184422

[20] M. T. Peracchia, E. Fattal, D. Desmaele, M. Besnard, J. P. Noel, J. M. Gomis, M. Appel, J. d'Angelo, and P. Couvreur, "Stealth pegylated polycyanoacrylate nanoparticles for intravenous administration and splenic targeting," *J Control Release*, vol. 60, no. 1, pp. 121–8, 1999. [Online]. Available: https://www.ncbi.nlm.nih.gov/pubmed/10370176

[21] G. Kaul and M. Amiji, "Long-circulating poly(ethylene glycol)-modified gelatin nanoparticles for intracellular delivery," *Pharm Res*, vol. 19, no. 7, pp. 1061–7, 2002. [Online]. Available: https://www.ncbi.nlm.nih.gov/pubmed/12180540

[22] L. Sanchez, Y. Yi, and Y. Yu, "Effect of partial pegylation on particle uptake by macrophages," *Nanoscale*, vol. 9, no. 1, pp. 288–297, 2017. [Online]. Available: https://www.ncbi.nlm.nih.gov/pubmed/27909711

[23] M. Viard, H. Reichard, B. A. Shapiro, F. A. Durrani, A. J. Marko, R. M. Watson, R. K. Pandey, and A. Puri, "Design and biological activity of novel stealth polymeric lipid nanoparticles for enhanced delivery of hydrophobic photodynamic therapy drugs," *Nanomedicine*, vol. 14, no. 7, pp. 2295–2305, 2018. [Online]. Available: https://www.ncbi.nlm.nih.gov/pubmed/30059754

[24] P. L. Rodriguez, T. Harada, D. A. Christian, D. A. Pantano, R. K. Tsai, and D. E. Discher, "Minimal "self' peptides that inhibit phagocytic clearance and enhance delivery of nanoparticles," *Science*, vol. 339, no. 6122, pp. 971–5, 2013. [Online]. Available: https://www.ncbi.nlm.nih.gov/pubmed/23430657

[25] F. Jivan, R. Yegappan, H. Pearce, J. K. Carrow, M. McShane, A. K. Gaharwar, and D. L. Alge, "Sequential thiol-ene and tetrazine click reactions for the polymerization and functionalization of hydrogel microparticles," *Biomacromolecules*, vol. 17, no. 11, pp. 3516–3523, 2016. [Online]. Available: https://www.ncbi.nlm.nih.gov/pubmed/27656910

[26] H. S. Han, N. K. Devaraj, J. Lee, S. A. Hilderbrand, R. Weissleder, and M. G. Bawendi, "Development of a bioorthogonal and highly efficient conjugation method for quantum dots using tetrazine-norbornene cycloaddition," *J Am Chem Soc*, vol. 132, no. 23, pp. 7838–9, 2010. [Online]. Available: https://www.ncbi.nlm.nih.gov/pubmed/20481508

[27] H. S. Han, E. Niemeyer, Y. Huang, W. S. Kamoun, J. D. Martin, J. Bhaumik, Y. Chen, S. Roberge, J. Cui, M. R. Martin, D. Fukumura, R. K. Jain, M. G. Bawendi, and D. G. Duda, "Quantum dot/antibody conjugates for in vivo cytometric imaging in mice," *Proc Natl Acad Sci U S A*, vol. 112, no. 5, pp. 1350–5, 2015. [Online]. Available: https://www.ncbi.nlm.nih.gov/pubmed/25605916

[28] Z. Huang, Y. Yang, Y. Jiang, J. Shao, X. Sun, J. Chen, L. Dong, and J. Zhang, "Anti-tumor immune responses of tumor-associated macrophages via toll-like receptor 4 triggered by cationic polymers," *Biomaterials*, vol. 34, no. 3, pp. 746–55, 2013. [Online]. Available: https://www.ncbi.nlm.nih.gov/pubmed/23107297

[29] J. Kim, H. Y. Kim, S. Y. Song, S. H. Go, H. S. Sohn, S. Baik, M. Soh, K. Kim, D. Kim, H. C. Kim, N. Lee, B. S. Kim, and T. Hyeon, "Synergistic oxygen generation and reactive oxygen species scavenging by manganese ferrite/ceria co-decorated nanoparticles for rheumatoid arthritis treatment," *ACS Nano*, 2019. [Online]. Available: https://www.ncbi.nlm.nih.gov/pubmed/30830763

[30] B. D. Fairbanks, M. P. Schwartz, C. N. Bowman, and K. S. Anseth, "Photoinitiated polymerization of peg-diacrylate with lithium phenyl-2,4,6-trimethylbenzoylphosphinate: polymerization rate and cytocompatibility," *Biomaterials*, vol. 30, no. 35, pp. 6702–7, 2009. [Online]. Available: https://www.ncbi.nlm.nih.gov/pubmed/19783300

[31] B. D. Fairbanks, M. P. Schwartz, A. E. Halevi, C. R. Nuttelman, C. N. Bowman, and K. S. Anseth, "A versatile synthetic extracellular matrix mimic via thiol-norbornene photopolymerization," *Adv Mater*, vol. 21, no. 48, pp. 5005–5010, 2009. [Online]. Available: https://www.ncbi.nlm.nih.gov/pubmed/25377720

[32] M. Muller, B. Kessler, J. Frohlich, S. Poeschla, and B. Torger, "Polyelectrolyte complex nanoparticles of poly(ethyleneimine) and poly(acrylic acid): Preparation and applications," *Polymers*, vol. 3, no. 2, pp. 762–778, 2011. [Online]. Available: ¡Go to ISI¿://WOS:000208601500006

[33] H. J. Je, E. S. Kim, J. S. Lee, and H. G. Lee, "Release properties and cellular uptake in caco-2 cells of size-controlled chitosan nanoparticles," *J Agric Food Chem*, vol. 65, no. 50, pp. 10 899–10 906, 2017. [Online]. Available: https://www.ncbi.nlm.nih.gov/pubmed/29172499

[34] M. Danaei, M. Dehghankhold, S. Ataei, F. Hasanzadeh Davarani, R. Javanmard, A. Dokhani, S. Khorasani, and M. R. Mozafari, "Impact of particle size and polydispersity index on the clinical applications of lipidic nanocarrier systems," *Pharmaceutics*, vol. 10, no. 2, 2018. [Online]. Available: https://www.ncbi.nlm.nih.gov/pubmed/29783687

[35] S. Eising, A. H. J. Engwerda, X. Riedijk, F. M. Bickelhaupt, and K. M. Bonger, "Highly stable and selective tetrazines for the coordination-assisted bioorthogonal ligation with vinylboronic acids," *Bioconjug Chem*, vol. 29, no. 9, pp. 3054–3059, 2018. [Online]. Available: https://www.ncbi.nlm.nih.gov/pubmed/30080405

[36] N. Platt, H. Suzuki, Y. Kurihara, T. Kodama, and S. Gordon, "Role for the class a macrophage scavenger receptor in the phagocytosis of apoptotic thymocytes in vitro," *Proc Natl Acad Sci U S A*, vol. 93, no. 22, pp. 12 456–60, 1996. [Online]. Available: https://www.ncbi.nlm.nih.gov/pubmed/8901603

[37] R. Heo, D. G. You, W. Um, K. Y. Choi, S. Jeon, J. S. Park, Y. Choi, S. Kwon, K. Kim, I. C. Kwon, D. G. Jo, Y. M. Kang, and J. H. Park, "Dextran sulfate nanoparticles as a theranostic nanomedicine for rheumatoid arthritis," *Biomaterials*, vol. 131, pp. 15–26, 2017. [Online]. Available: https://www.ncbi.nlm.nih.gov/pubmed/28371624

[38] P. H. Wu, Y. Onodera, Y. Ichikawa, E. B. Rankin, A. J. Giaccia, Y. Watanabe, W. Qian, T. Hashimoto, H. Shirato, and J. M. Nam, "Targeting integrins with rgd-conjugated gold nanoparticles in radiotherapy decreases the invasive activity of breast cancer cells," *Int J Nanomedicine*, vol. 12, pp. 5069–5085, 2017. [Online]. Available: https://www.ncbi.nlm.nih.gov/pubmed/28860745

[39] T. G. Kapp, F. Rechenmacher, S. Neubauer, O. V. Maltsev, E. A. Cavalcanti-Adam, R. Zarka, U. Reuning, J. Notni, H. J. Wester, C. Mas-Moruno, J. Spatz, B. Geiger, and H. Kessler, "A comprehensive evaluation of the activity and selectivity profile of ligands for rgd-binding integrins," *Sci Rep*, vol. 7, p. 39805, 2017. [Online]. Available: https://www.ncbi.nlm.nih.gov/pubmed/28074920

[40] K. Cherukula, S. Uthaman, and I. K. Park, "Design of an amphiphilic poly(aspartamide)-mediated self-assembled nanoconstruct for long-term tumor targeting and bioimaging," *Molecules*, vol. 24, no. 5, 2019. [Online]. Available: https://www.ncbi.nlm.nih.gov/pubmed/30832383

[41] T. J. Bartosh and J. H. Ylostalo, "Macrophage inflammatory assay," *Bio Protoc*, vol. 4, no. 14, 2014. [Online]. Available: https://www.ncbi.nlm.nih.gov/pubmed/27570796

[42] D. A. Chistiakov, V. A. Myasoedova, V. V. Revin, A. N. Orekhov, and Y. V. Bobryshev, "The impact of interferon-regulatory factors to macrophage differentiation and polarization into m1 and m2," *Immunobiology*, vol. 223, no. 1, pp. 101–111, 2018. [Online]. Available: https://www.ncbi.nlm.nih.gov/pubmed/29032836

[43] Y. Kono, S. Miyoshi, and T. Fujita, "Dextran sodium sulfate alters cytokine production in macrophages in vitro," *Pharmazie*, vol. 71, no. 11, pp. 619–624, 2016. [Online]. Available: https://www.ncbi.nlm.nih.gov/pubmed/29441964

APPENDICES

APPENDIX A. REPORTED NP CHARACTERISTICS

Table A.1: Table of Material Characteristics, NP Mixing Method, and Reported Size of Hep/PLL PEC NPs [11–17].

Agitation Method	Size	PLL MW	Heparin MW	Citation
Not reported	Not reported	3kDa	4.5kDa	[11]
Ultrasonic Condition	200-1175nm	150-300kDa	Less than 8kDa	[12]
Ultrasonic Condition	389nm	150-300kDa	Less than 8kDa	[13]
Stirring	246nm	3.2-4.5kDa	6-20kDa	[14]
Ultrasonic Condition	399nm	150-300kDa	Less than 8kDa	[15]
Stirring	160-230nm	4-7kDa	Not Reported	[16]
Ultrasonic Condition	189-327nm	150-300kDa	Less than 8kDa	[17]

APPENDIX B. ADDITIONAL NP CHARACTERIZATION

Table B.1: NPs Prepared with Different Concentrations.

[Hep]/[PLL]	[Hep] mg/mL	Zeta Potential (mV)	Size (nm)	PDI
1.3	0.325	-50.6±0.6	123.2±5.2	0.149±0.011
1.3	2.000	-46.0±0.6	157.1±6.1	0.174±0.015

Table B.2: DLS Measurements of 2 Step NPs with Different Layered Polyanions. PLL concetration of 0.250 mg/mL.

Layered Polymer	Zeta Potential (mV)	Size (nm)	PDI
Hep	-50.6 ± 0.6	123.2 ± 5.2	0.149 ± 0.011
Hep-Tz	-46.8 ± 1.1	133.4 ± 3.2	0.136 ± 0.006
Hep-mTz	-42.6 ± 2.5	137.6 ± 2.1	0.126 ± 0.004
Dex	-51.9 ± 1.9	134.2 ± 0.8	0.144 ± 0.007

APPENDIX C. CELLULAR UPTAKE

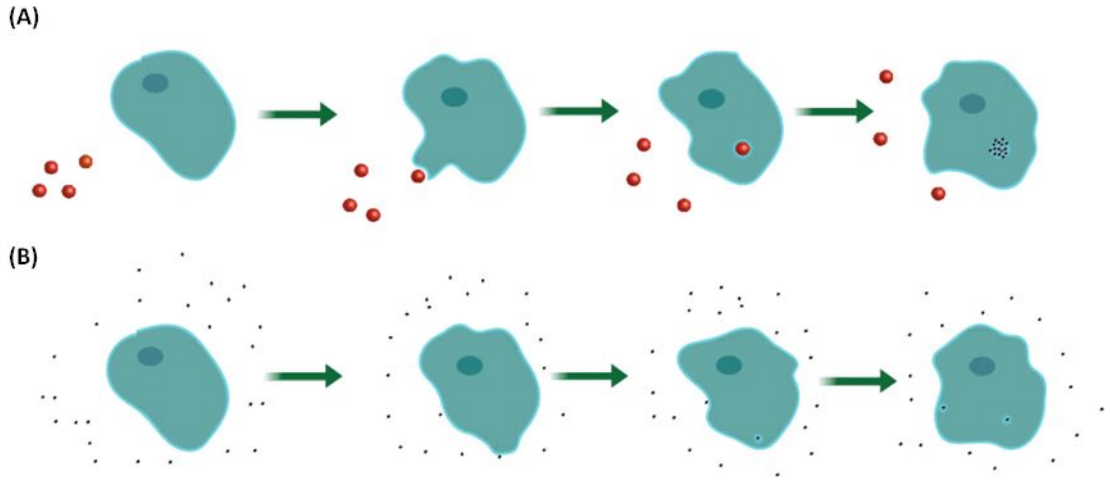

Fig. C.1: Schematic representation of cellular uptake of (A) DS coated NPs and (B) soluble DS. Soluble DS shown in black. Soluble PLL and Hep are not included.